Molecular Biology and Evolution, 2025, **42**, 1–20
https://doi.org/10.1093/molbev/msaf100
Advance access publication 7 May 2025
Discoveries

MBE OXFORD

Comparative Phylogenetics Reveal Clade-specific Drivers of Recombination Rate Evolution Across Vertebrates

Taylor Szasz-Green [1,*] **Katherynne Shores** [1] **Vineel Vanga** [1] **Luke Zacharias** [1] **Andrew K. Lawton** [2] **Amy L. Dapper** [1]

[1]Department of Biological Sciences, Mississippi State University, Mississippi State, MS 39762, USA
[2]Department of Biology, Appalachian State University, Boone, NC 28608, USA

***Corresponding author:** E-mail: ts748@msstate.edu.**Associate editor**: Emily Josephs

Abstract

Meiotic recombination is an integral cellular process, required for the production of viable gametes. Recombination rate is a fundamental genomic parameter, modulating genomic responses to selection. Our increasingly detailed understanding of its molecular underpinnings raises the prospect that we can gain insight into trait divergence by examining the molecular evolution of recombination genes from a pathway perspective, as in mammals, where protein-coding changes in later stages of the recombination pathway are connected to divergence in intra-clade recombination rate. Here, we leverage increased availability of avian and teleost genomes to reconstruct the evolution of the recombination pathway across two additional vertebrate clades: birds, which have higher and more variable rates of recombination and similar divergence times to mammals, and teleost fish, which have much deeper divergence times. Rates of molecular evolution of recombination genes are highly correlated between vertebrate clades and significantly elevated compared to control panels, suggesting that they experience similar selective pressures. Avian recombination genes are significantly more likely to exhibit signatures of positive selection than other clades, unrestricted to later stages of the pathway. Signatures of positive selection in genes linked to recombination rate variation in mammalian populations and those with signatures of positive selection across the avian phylogeny are highly correlated. In contrast, teleost fish recombination genes have significantly less evidence of positive selection despite high intra-clade recombination rate variability. Gaining clade-specific understanding of patterns of variation in recombination genes can elucidate drivers of recombination rate and thus, factors influencing genetic diversity, selection efficacy, and species divergence.

Keywords: meiotic recombination, molecular evolution, comparative phylogenetics

Introduction

Although meiotic recombination, the exchange of genetic material between homologous chromosomes is ubiquitous in sexually reproducing organisms, the rate at which it occurs varies significantly within and between species (Stapley et al. 2017). This variation has wide-ranging consequences: Recombination generates new combinations of alleles within populations, shaping patterns of genetic variation within and between genomes and modulating the efficacy of selection (Hill and Robertson 1966; Charlesworth et al. 1993). Recombination rate can also directly impact zygote viability. In most species, a minimum of one crossover event per chromosome pair is required to ensure the resulting gametes each receive the proper genetic complement (Baker et al. 1976).

Proximally, recombination rate is determined by the number of crossover events, which arise through a highly-regulated and complex cellular pathway (Dapper and Payseur 2019). While there are still large gaps in our understanding of how and why recombination diverges between species, it is likely that variation in the genes that regulate the meiotic recombination pathway are important contributors (Kong et al. 2008; Chowdhury et al. 2009; Sandor et al. 2012; Johnston et al. 2016; Kadri et al. 2016; Shen et al. 2018). Thus, one strategy for understanding how species diverge is to inspect molecular evolution of genes involved in this pathway.

The meiotic recombination pathway can be divided up into discrete steps (Meuwissen et al. 1992; Baker et al. 1996; Keeney et al. 1997; Page and Hawley 2004; Snowden et al. 2004; Keeney 2008). Previous research in mice, yeast, and nematodes identified roughly six stages in the meiotic recombination pathway and key genes acting on each step (Fig. 1). In mammals, two lines of evidence connect protein-coding changes in later stages of the pathway to differences in rates of recombination. First, within populations, individual variation in recombination rate is linked to genetic variation at key loci in the recombination pathway (Dumont et al. 2009). Genetic variants that impact recombination rate within species have been identified in humans, pigs, cattle, sheep, and red deer (Kong et al. 2008; Sandor et al. 2012; Johnston et al. 2016, 2018; Kadri et al. 2016; Petit et al. 2017; Halldorsson et al. 2019; Brekke et al. 2022). The majority of these gene variants are found in the latter half of the recombination pathway, regulating which double strand breaks are resolved as crossovers. Second, Dapper and Payseur identified signatures of positive selection in a focal panel of meiotic recombination genes within mammals (Dapper and Payseur 2019). Specifically, genes involved with the stabilization of homologous pairing and the

Received: June 28, 2024. **Revised:** March 6, 2025. **Accepted:** April 11, 2025

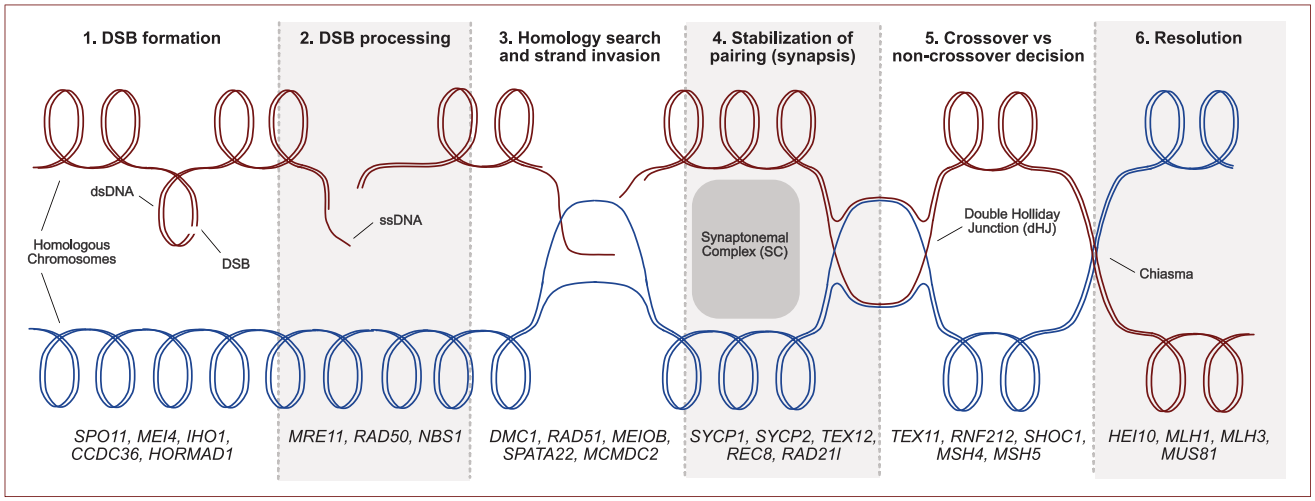

Fig. 1. The meiotic recombination pathway can be broken down into six steps. (1) First, double-stranded breaks (DSBs) are non-randomly introduced throughout the genome. (2) Once these breaks are introduced, they are processed via nucleases, which leave each DSB with an ssDNA tail. (3) These tails allow DSBs to be lined up appropriately along homologous chromosomes via homology search and strand invasion. (4) The synaptonemal complex (SC) forms a proteinacious scaffold that stabilizes DSBs and homologous chromosomes and creates a structure on which crossover events occur. (5) Though the majority of DSBs are resolved as non-crossovers, a non-randomly distributed subset of the DSBs are designated as crossovers. (6) Finally, DNA repair occurs on both crossovers and non-crossovers, resolving all DSBs. Key genes that regulate each step are listed at the bottom of the figure. Figure modified from Dapper and Payseur (2019).

crossover/non-crossover (CO/NCO) decision showed greater likelihood of signatures of adaptive evolution, supporting the hypothesis that changes to genes associated with the CO/NCO decision drive divergence in recombination rate between populations (Martini et al. 2006; Cole et al. 2012).

An important consideration in examining the evolution of the recombination pathway outside of mammals is that most work uncovering the genetics and cellular mechanisms of meiotic recombination has been carried out in model organisms, such as yeast, Caenorhabditis elegans, and the house mouse. However, the deep conservation of pathway elements between these distantly related model organisms suggests that we may be able to infer gene function in non-model organisms with some confidence (Kanaar et al. 1996; Bergerat et al. 1997; Cole et al. 2010; Kumar et al. 2010; Kan et al. 2011; de Massy 2013; Loidl 2016; Zelkowski et al. 2019; Hinman et al. 2021).

Due to their higher recombination rate variability, avian and teleost genomes may afford greater power to identify correlations between molecular evolution and divergence in recombination rates, providing a strong test of the hypothesis that changes to the genes that regulate later stages of the recombination pathway drive divergence in recombination rate between vertebrate genomes. Yet, there are also interesting genomic distinctions between these clades that may result in different selective pressures shaping the evolution of recombination rate and its regulatory pathway. Unlike mammalian and teleost genomes, avian genomes contain numerous microchromosomes, <0.5 μm diameter chromosomes that each require a recombination event to segregate properly (Solovei et al. 1994; Waters et al. 2021). Additionally, PRDM9, a key, rapidly evolving gene directs recombination hotspots in most mammalian and some teleost genomes (Baudat et al. 2010; Myers et al. 2010; Parvanov et al. 2010; Auton et al. 2013; Zhou et al. 2018; Raynaud et al. 2025). But, it is notably absent in avian, yeast, and plant genomes (Oliver et al. 2009; Baker et al. 2017; Cavassim et al. 2022). Despite the loss of PRDM9, leading to stable recombination hotspots in avians (Singhal et al. (2015), we find evidence of large genome and chromosome-wide variation in recombination rate. These significant differences in recombination mechanism underlie the importance of investigating meiotic recombination rate evolution in non-model, and specifically non-mammalian, organisms.

While major drivers of the evolution of meiotic recombination genes have yet to be determined, several hypotheses provide motivation for deeper investigation into the selective landscape of recombination rate variation. Because recombination events play an important role in proper chromosomal segregation during meiosis, karyotype evolution may drive repeated bouts of selection on recombination rate (Kong et al. 2004; Ritz et al. 2017; Dapper and Payseur 2017). Karyotypic evolution in birds, while largely stable, produced massive variation in number of chromosomes between bird clades, with diploid chromosome numbers varying between 40 and 142 (Degrandi et al. 2020). Both birds and mammals have experienced significant chromosome rearrangement events, leading to significant variation in karyotype structure between species (Ferguson-Smith and Trifonov 2007). While mammalian chromosomes retain large conserved segments, bird chromosomes have experienced frequent, independently occurring chromosome fusions and fissions, leading to varying numbers of microchromosomes (Ferguson-Smith and Trifonov 2007; Graphodatsky et al. 2011; Kapusta et al. 2017; Degrandi et al. 2020; Damas et al. 2022; Huang et al. 2022). Additionally, birds have shorter genomes, introns, and intergenic regions than mammals, potentially due to chromosomal rearrangements (Botero-Castro et al. 2017). Mammals and birds have "elastic" genomic architectures due to complicated patterns of DNA gain and loss (Kapusta et al. 2017). Teleost fish have also experienced significant karyotypic evolution due to a whole genome duplication, subsequent rediploidization, and loss/partitioning of gene duplicates (Jaillon et al. 2004; Volff 2005; Parey et al. 2022). These significant changes in karyotype and genomic architecture may drive directional selection on recombination rate to ensure the one-crossover rule is maintained, and to

compensate for potential downstream effects of chromosomal rearrangements. Meiotic drive and indirect effects on other, linked loci may also generate recurrent directional selection on recombination rate (Brandvain and Coop 2012). Meiotic drivers occur frequently in females, as the unequal division in gametes may result in drivers preferentially segregating to the oocyte, with other loci being relegated to the polar bodies (Brandvain and Coop 2012). Genetic conflict can thus arise between drivers and other loci; this conflict may be mediated by selection on recombination rate modifiers, which can neutralize the efficacy of meiotic drivers. Similar to the conflict between meiotic drivers and other loci, theory also predicts that inter-locus sexual conflict can also generate recurrent selection on recombination rate (Dapper and Lively 2014). Strong directional selection on other traits is another plausible indirect driver of adaptive evolution on meiotic recombination genes. Research in *Drosophila melanogaster* identified a relationship between increased recombination rate and polygenic development of DDT resistance (Flexon and Rodell 1982). In plants, inter-species analysis reveals higher rates of recombination in domesticated taxa (Ross-Ibarra 2004), though there is less consensus on the relationship between domesticity and recombination rate in mammals and birds (Burt and Bell 1987; Otto and Barton 2001; Martin et al. 2006; Muñoz-Fuentes et al. 2015). In mice and humans, there is an association between higher recombination rates and fecundity (Gorlov et al. 1992; Kong et al. 2004). While these traits are not specific to meiotic recombination, it is possible that directional selection acting on beneficial alleles is linked to variants associated with recombination rate variation, such as those previously mentioned in humans and livestock (Kong et al. 2008; Sandor et al. 2012; Johnston et al. 2016, 2018; Kadri et al. 2016; Petit et al. 2017; Halldorsson et al. 2019; Brekke et al. 2022). Birds provide a strong comparative system for investigating patterns of molecular evolution in the meiotic recombination pathway. Both birds and placental mammals have divergence times of ~100 million years (Jarvis et al. 2014; Claramunt and Cracraft 2015; Prum et al. 2015; Dunwell et al. 2017; Liu et al. 2017; Kuhl et al. 2021; Carlisle et al. 2023). Avian diversity is well-represented by an array of high-quality genome assemblies. Interestingly, avian genomes appear to experience recombination rates that are on average twice as high as those observed in mammals (Ellegren 2010; Stapley et al. 2017) with greater between-species divergence, but higher karyotypic conservation (Ellegren 2010; Zhang et al. 2014; Kapusta et al. 2017). Teleost fish provide an interesting foil to both mammal and avian meiotic recombination pathway evolution. Linkage map length data suggest that fish have both the highest and lowest recombination rates across vertebrates while still maintaining an average recombination rate twice that of mammals (Stapley et al. 2017). However, it is important to note that teleost fish also have a divergence time over twice that of mammals and birds (Takezaki 2018; Cooney et al. 2021).

Here, we use a comparative phylogenetic framework to measure the rates of molecular evolution and identify signatures of positive selection within a panel of key genes in the recombination pathway in avian and teleost clades. Because avian and teleost genomes exhibit higher and more variable recombination rates, we hypothesize that key recombination genes are experiencing elevated rates of molecular evolution and significant signatures of adaptive evolution, as expected of these differences in recombination rate between mammals, teleosts and birds. Therefore, we predict to see signatures of positive selection within genes driving the CO/NCO decision and synapsis of homologous chromosomes and thus, an association between positively selected genes and genes associated with recombination rate variation. We address the following questions: (i) Do recombination genes evolve more rapidly in non-mammals? (ii) Is there more evidence of positive selection in recombination pathway genes in other clades? (iii) What patterns of molecular evolution influence recombination rate variation in birds and teleost fish? (iv) Are bird and teleost fish recombination genes with signatures of selection also associated with variation in recombination rate? Understanding how patterns of variation in recombination genes differ between clades provides valuable insight into the drivers of recombination rate and thus, the forces governing genetic diversity, selection efficacy, and species divergence.

Results

Bird and Teleost Genomes Have Higher and More Variable Rates of Recombination Than Mammals

While previous studies have found that avian recombination rates are approximately double those observed in mammals, these comparisons do not control for important karyotypic differences between mammalian and avian genomes (Ellegren 2010; Stapley et al. 2017). More specifically, avian genomes contain numerous microchromosomes, in addition to macrochromosomes similar to those found in mammalian genomes. Since each microchromosome requires a minimum of one crossover to properly segregate (Ellegren 2010), the extended genetic map length observed in avian genomes could be due to karyotypic differences alone. In other words, the differences in recombination rate could stem from differences in chromosome size and number, rather than differences in the cellular regulation of the number of crossovers. To determine whether recombination rates in avian genomes are higher than those observed among mammals, when taking karyotype into account, we performed a meta-analysis of published cytological (MLH1) studies of recombination rates in avian and mammalian genomes (supplementary file S1, Supplementary Material online). We also leveraged previously published estimates of genetic map length in teleost fish (supplementary file S1, Supplementary Material online) to compare recombination rate measured as cM/Mb and XO/HCN between all three clades, due to teleosts' lack of microchromosomes and high recombination rates.

We first compared genome-wide measures of recombination rate between avian, teleost, and mammalian clades, measured in cM/Mb (estimated from MLH1 and linkage map data) and in crossovers per haploid chromosomes number (XO/HCN). While birds and teleosts have significantly higher recombination rates when measured as cM/Mb than mammalian genomes (Fig. 2a, $P < 0.0001$, Wilcoxon rank sum test), confirming previous reports, we did not find a significant difference between genome-wide recombination rates between these three clades when measured as XO/HCN (Fig. 2b, $P > 0.05$, Wilcoxon rank sum test). In fact, the trend is towards avian and teleost genomes having fewer crossovers per chromosome pair than mammalian genomes. However, both comparisons fail to isolate differences in regulation of recombination rate from karyotypic differences. Just as microchromosomes may increase recombination rate when measured as cM/Mb, they are expected to depress measures of genome-wide

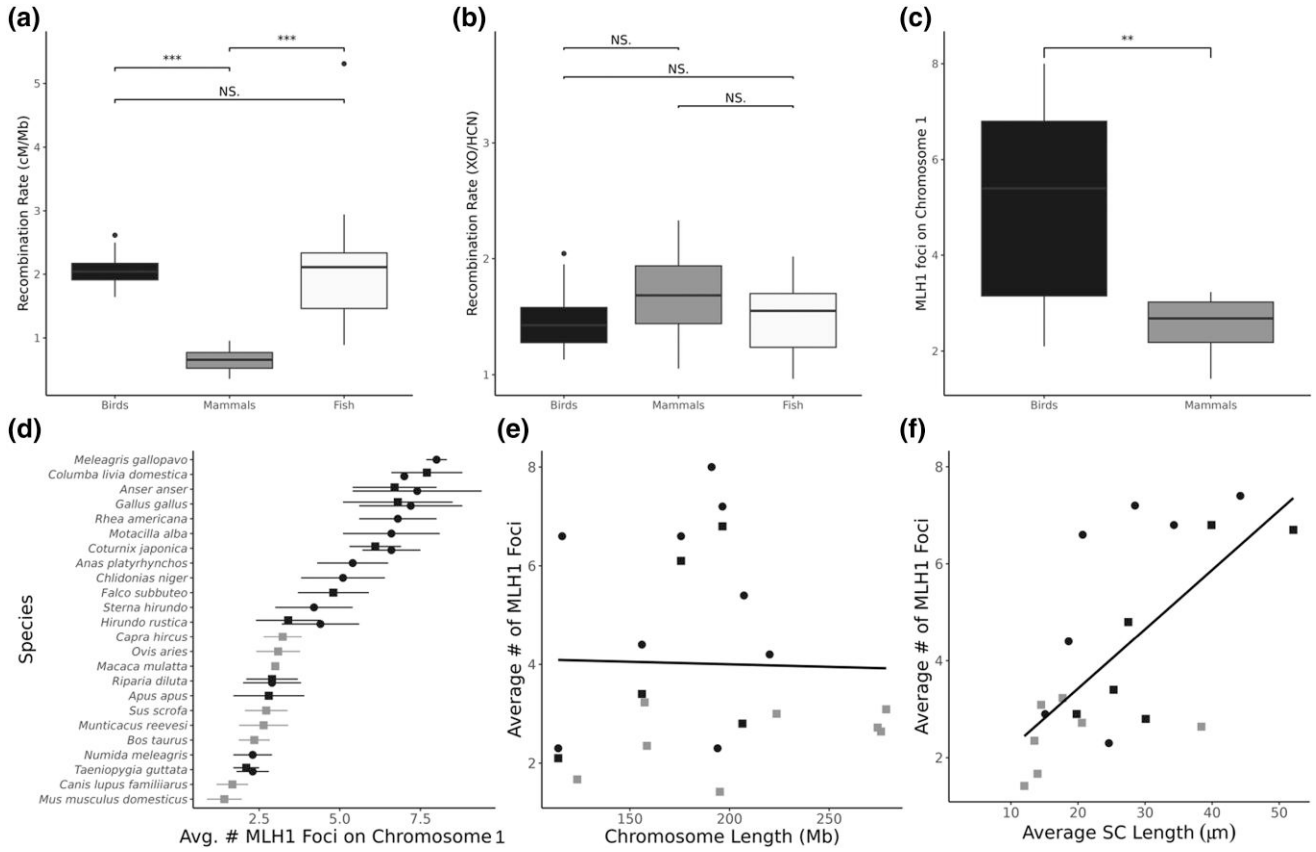

Fig. 2. a) Recombination rate differences between birds, mammals and teleosts measured as cM/Mb (*** = $P < 0.0001$). b) Recombination rate differences between birds, mammals and teleosts measured as XO/HCN (crossovers per haploid chromosome number; $P = 0.1628$). c) Comparison of number of MLH1 foci on chromosome 1 in birds and mammals (* = $P < 0.05$). d) Species-level comparison of average number of MLH1 foci on chromosome 1 between birds (black) and mammals (grey) by sex, where females are circles and males are squares. There are no female data for mammals. e) Correlation between length of chromosome 1 and average number of MLH1 foci on chromosome 1 ($R^2 = 0.0006$, $P = 0.9115$, linear regression). f) Correlation between average synaptonemal complex length and average number of MLH1 foci on chromosome 1 between mammals and birds ($R^2 = 0.46$, $P = 0.001$, linear regression). Species used for each comparison are available in supplementary file S1, Supplementary Material online.

recombination when measured as XO/HCN. To better determine whether avian genomes differ from their mammalian counterparts in recombination rate at the chromosomal scale, we compared the average number of MLH1 foci, a proxy for the number of crossover events, on chromosome 1—by convention, the largest chromosome in the genome. Teleost fish were not included in this analysis due to a paucity of MLH1 foci analyses in this clade. When measured this way, we found higher and more variable recombination rates among avian genomes (Fig. 2c and d, $P = 0.0108$, t-test). There is no correlation between the physical size of chromosome 1 and average number of crossovers (Fig. 2e, $R^2 = 0.0006$, $P = 0.91$, linear regression). This is exemplified by comparing largest chromosome in the mouse and chicken genomes. While they are both exceedingly similar in physical size (197 vs. 195 Mbps, respectively), the largest chicken chromosome has on average 9 MLH1 foci, while the largest mouse chromosome has on average 1.4 MLH1 foci (Anderson et al. 1999; Pigozzi 2001; Nam et al. 2010). Importantly, heterochiasmy is not implicated in the differences uncovered in our dataset, allowing us to make cross sex comparisons. There was no significant difference in avian sex-specific recombination rate when measured as cM/Mb ($P = 0.5579$), XO/HCN ($P = 0.1175$), or MLH1 foci on chromosome 1 ($P = 0.4764$; supplementary fig. S1, Supplementary Material online). Restricting our analyses to only male data from birds and mammals did not impact the results (supplementary fig. S2, Supplementary Material online). Interestingly, the length of the synaptonemal complex (SC) is considerably longer relative to physical chromosome size in birds than in mammals ($P = 0.044$, paired t-test) and is significantly correlated with recombination rate (Fig. 2f, $R^2 = 0.46$, $P = 0.001$, linear regression). This clearly suggests that changes to the proteins in the recombination pathway, specifically those that regulate and/or form the SC, may be responsible for the differences in patterns of recombination between these clades and motivates a comparative analysis of the molecular evolution of the recombination pathway.

Recombination Genes are Evolving Rapidly in Avians, Mammals, and Teleost Fish

If the higher and more variable rates of recombination in the avian and teleost clades are due to molecular changes in the underlying pathway, we might expect that genes regulating the recombination pathway have evolved more rapidly in the avian and teleost clades than the mammalian clade. To test this prediction, we used PAML (Yang 2007) to measure the molecular evolutionary rate, represented by ω, of a panel of 29 key recombination genes across the avian phylogeny (Fig. 3a, supplementary tables S1 and S2, Supplementary Material online) and compared these estimates to those reported for the orthologous genes across the mammalian phylogeny in Dapper and Payseur (2019) (supplementary table S3, Supplementary Material online). We found that the

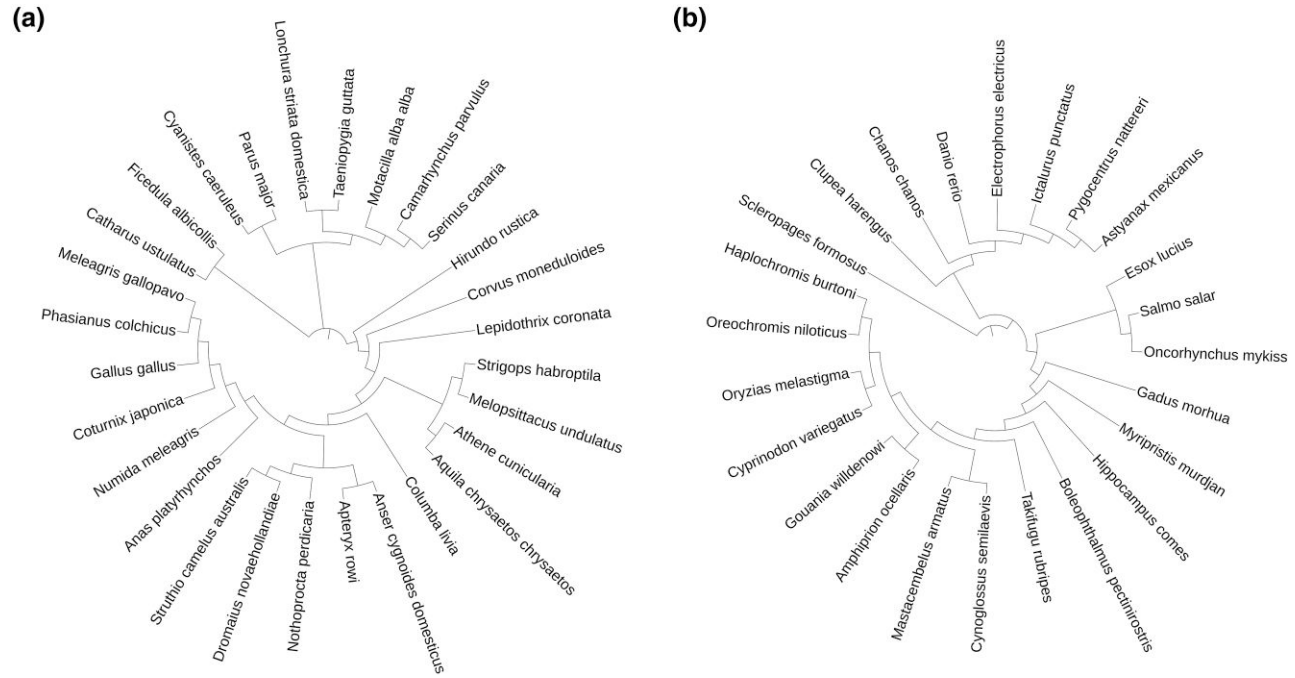

Fig. 3. Species tree for birds a) and teleost fish b) used for analysis of molecular evolution in bird and teleost fish recombination genes. Teleost fish phylogeny also includes basal teleost Scleropages formosus. Figure generated using Letunic and Bork (2021).

evolutionary rates of focal genes across the avian phylogeny ranged from 0.0137 to 0.5778 (mean $\omega = 0.3123$, SD = 0.1606, median = 0.3021; Fig. 4a, Table 1). Within mammals, ω values ranged from 0.0268 to 0.8483 (mean $\omega = 0.3275$, SD = 0.1971, median = 0.3095; Dapper and Payseur 2019). In comparison with mammals, the average rate of evolution of avian recombination genes is quite similar, and birds show no significant difference in the distribution of ω values ($\omega_{Bird} = 0.3123$, $\omega_{Mammal} = 0.3275$, $P = 0.7718$, Wilcoxon rank sum test; Fig. 4a).

Teleost, or ray-finned fishes, diverged from the tetrapod lineage between 350 and 400 million years ago (Near et al. 2012). Notably, teleost fish broadly lack microchromosomes and thus have a similar chromosomal structure to mammals. Yet, meta-analyses of genetic maps show they have higher and more variable rates of recombination than mammals (when measured as cM/Mb; Fig. 2a; Stapley et al. 2017). Though, it is noteworthy that our meta-analysis did not find significant differences when comparing the average number of crossovers per chromosome (XO/HCN, Fig. 2b). Thus, we may predict to also observe similarly elevated rates of evolution of the recombination pathway across the teleost clade. To test this prediction, we again used PAML (Yang 2007) to measure the molecular evolutionary rate, represented by ω, of the panel of 28 key recombination genes across the teleost and basal teleost phylogeny (Fig. 3b, supplementary table S4, Supplementary Material online). TEX12 was not consistently identified in teleosts and was thus left out. Molecular evolution of recombination genes across the teleost phylogeny ranged from 0.0272 to 0.3952 (mean $\omega = 0.2122$, SD = 0.0967, median = 0.2138, supplementary tables S5 and S6, Supplementary Material online).

In order to determine if rates of molecular evolution of recombination genes were significantly elevated within each clade, we compared ω values to two control panels: (1) genes involved in the SHH brain development pathway and (2) neighboring genes found up or downstream of our focal panel. Strikingly, in all three clades, there is a significant difference in the mean ω between recombination genes and both control panels (Table 2), despite overall lower ω values in teleosts (Fig. 4a). There was no significant difference in rates of molecular evolution between brain and up/downstream genes for all clades after multiple testing correction (Table 2, P Bird = 0.6462, P Mammal = 0.7215, P Fish = 0.1232, ANOVA/Tukey HSD).

The Recombination Pathway is Experiencing Similar Selective Pressures Across Vertebrates

If the recombination pathway experiences similar selective pressures in vertebrate genomes, we predict that the rate of evolution between orthologous genes will be highly correlated across all three clades. Conversely, striking differences in evolutionary rates between clades may indicate genes, or steps within the pathway, which are experiencing divergent selection pressures. We found that omega (ω) values for each gene are significantly correlated between birds and mammals, supporting the prediction that they have experienced similiar selection pressures ($R^2 = 0.58$, $P < 0.0001$, linear regression; Fig. 4c). Despite overall lower evolutionary rates of recombination genes in teleosts (Fig. 4a), we still observed a significant correlation in ω values between birds and teleosts ($R^2 = 0.599$, $P < 0.0001$, linear regression) and mammals and teleosts ($R^2 = 0.577$, $P < 0.0001$, linear regression; Fig. 4d and e), indicating that overall the pathway is experiencing similar selective landscapes. Consistent with this overall trend, there is considerable overlap between the most conserved and most rapidly evolving genes in the pathway between clades (Table 3). Key recombination genes exhibit striking differences in evolutionary rate among clades. Despite the overall concordance between evolutionary rates of recombination genes across the avian and mammalian phylogeny, *TEX11*, a gene whose evolutionary rate is positively correlated with recombination rate in mammals (Dapper and Payseur 2019), shows distinctly different evolutionary patterns in the two clades. While *TEX11* has an

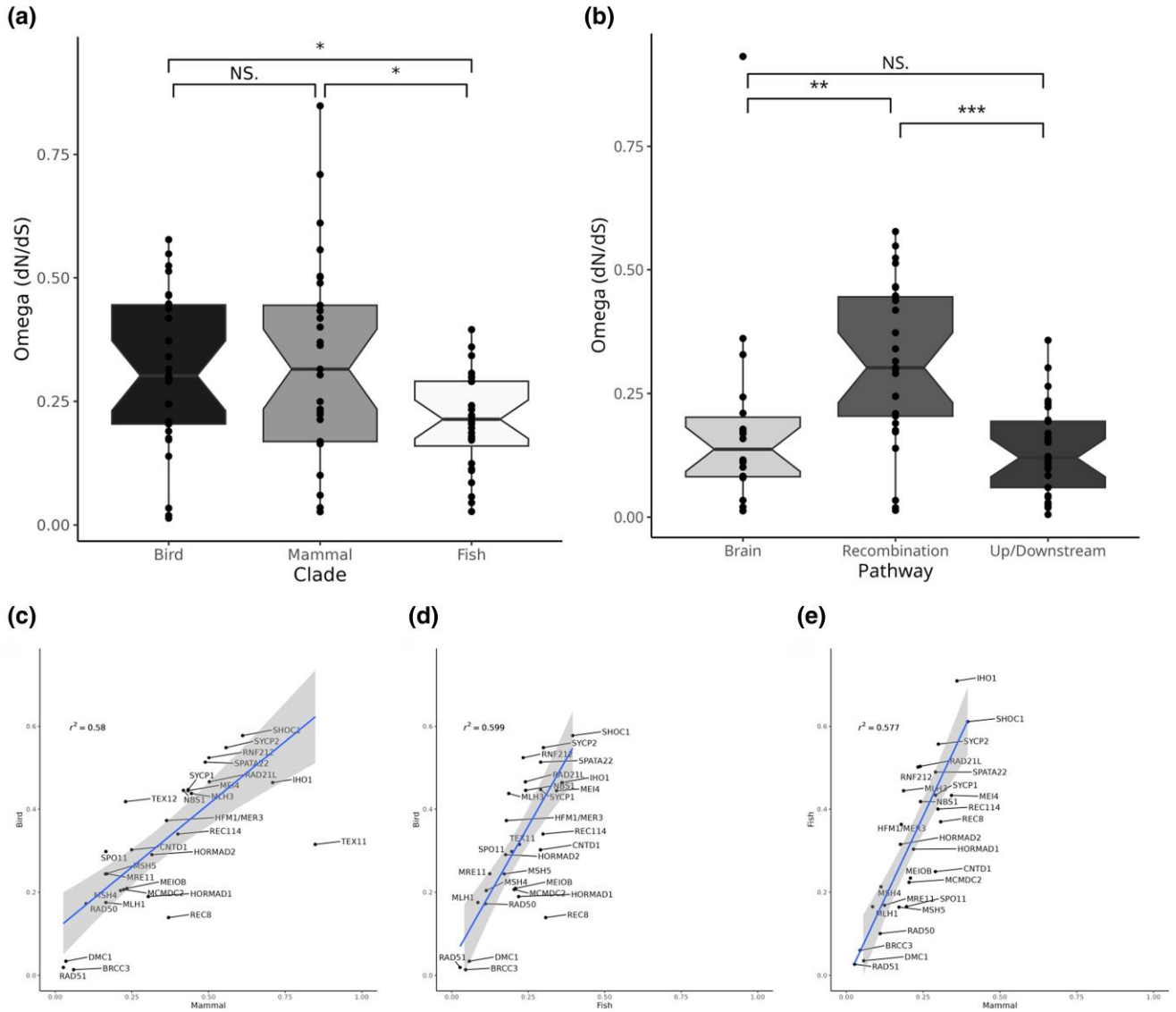

Fig. 4. a) Distribution of evolution rates of recombination genes between birds, teleost fish, and mammals (* = $P < 0.05$). b) Distribution of evolution rates between genes in the SHH (brain development), up/downstream and recombination gene panels in birds (** = $P < 0.01$, *** = $P < 0.0001$). c to e) Correlation of recombination pathway-associated gene omega values between c) Birds and mammals ($R^2 = 0.58$), d) Birds and teleost fish ($R^2 = 0.599$), and e) Teleost fish and mammals ($R^2 = 0.577$). Grey shading represents the 95% confidence interval for the linear regression.

ω value of >2 SD above the mean in mammals ($\omega_{TEX11} = 0.8483$), its evolutionary rate is nearly identical to the mean in birds ($\omega_{TEX11} = 0.3152$) and in teleosts ($\omega_{TEX11} = 0.2217$). Notably, *TEX11* is the only recombination gene identified as an influential point through Cook's distance (supplementary fig. S5a to c, Supplementary Material online, $D = 2.06$, threshold = 0.5; Cook 1977). As follows, the correlation between avian and mammalian ω values increases considerably with the removal of *TEX11* ($R^2 = 0.759$, $P < 0.0001$, linear regression), as does the correlation between teleost and mammalian ω values ($R^2 = 0.749$, $P < 0.0001$, linear regression). However, *TEX11* is only an influential point in comparisons between birds and mammals.

The Avian Recombination Pathway Exhibits Evidence of Elevated Rates of Positive Selection

Dapper and Payseur (2019) identified evidence of positive selection in 11 recombination genes across the mammalian phylogeny, significantly concentrated in the steps of the pathway that regulate synapsis and the crossover/non-crossover decision. If the increased variation in recombination rate in the avian clade is adaptive, we predict that we may observe more evidence of positive selection on genes underlying variation in this trait. If the pathway responds to selection in a predictable manner, we also predict that this adaptive evolution will be concentrated in avian recombination genes associated with the same steps of the pathway.

As predicted, we observed significantly more genes exhibiting signatures of positive selection in birds than in mammals ($P = 0.0214$, Fisher's exact test; Table 1). More specifically, we identified signatures of positive selection in 19 of 29 (65.5%) recombination genes in birds: *MEI4*, *REC114*, *IHO1*, *SPO11*, *MRE11*, *NBS1/NBN*, *SPATA22*, *REC8*, *RAD21L*, *SYCP1*, *SYCP2*, *TEX11*, *SHOC1*, *RNF212*, *MSH4*, *MSH5*, *HFM1/MER3*, *CNTD1*, and *MLH3*. Of those genes with signatures of positive selection, 16 identified potential codon sites impacted by positive selection (BEB, $P > 95\%$; Table 1). However, there is no significant difference between birds and mammals for either number of codon sites identified

Table 1 Evolutionary rates and tests for positive selection across birds at 29 recombination genes, including likelihood ratio tests for each model, average omega across the gene, and number of codon sites potentially experiencing positive selection (BEB, $P > 95\%$)

Gene	bp	N	omega	M	M1-M2	P	M7-M8	P	M8a-M8	P	BEB
A) DSB formation											
HORMAD1	1908	29	0.19	7	0	1	0	1	…	…	0
MEI4	1724	29	0.44	**8**	10.86	**0**	14.48	**0**	6.96	**0.01**	**1**
REC114	1776	29	0.34	**8**	4.14	0.13	17.23	**0**	6.81	**0.01**	**1**
IHO1	3133	24	0.46	**8**	9.77	**0.01**	17.29	**0**	10.09	**0**	**1**
SPO11	3525	29	0.3	**8**	14.26	**0**	30.4	**<0.0001**	16.26	**0**	**4**
B) DSB processing											
HORMAD2	1383	27	0.29	7	0	1	5.22	0.07	…	…	0
MRE11	2103	28	0.24	**8**	10.46	**0.01**	27.48	**<0.0001**	11.94	**0**	**1**
NBS1	2533	29	0.45	**8**	6.5	**0.04**	18.29	**0**	5.67	**0.02**	0
RAD50	4395	29	0.17	8a	0	1	28.17	**<0.0001**	1	0.32	0
BRCC3	1444	29	0.01	7	0	1	0	1	…	…	0
C) Homology search and strand invasion											
DMC1	1868	29	0.03	7	0	1	1.76	0.41	…	…	0
RAD51	1387	29	0.02	7	0	1	0	1	…	…	0
SPATA22	2398	29	0.51	**8**	12.75	**0**	22.39	**<0.0001**	15.9	**0**	**3**
MEIOB	2088	29	0.21	8a	0	1	7.89	**0.02**	2.22	0.14	0
MCMDC2	3566	29	0.21	7	0	1	2.95	0.23	…	…	0
D) Synapsis											
REC8	2571	29	0.14	**8**	17.21	**<0.0001**	37.63	**<0.0001**	22.99	**<0.0001**	**6**
RAD21L	2906	29	0.47	**8**	0.76	0.68	10.08	**0.01**	4.38	**0.04**	0
SYCP1	3577	26	0.45	**8**	21.22	**<0.0001**	47.48	**<0.0001**	17.06	**<0.0001**	**6**
SYCP2	5508	26	0.55	**8**	25.43	**<0.0001**	65.19	**<0.0001**	32.09	**<0.0001**	**5**
TEX12	1162	29	0.42	7	0	1	1.33	0.51	…	…	0
E) CO/NCO decision											
TEX11	4555	29	0.32	**8**	17.87	**<0.0001**	41.21	**<0.0001**	12.25	**0**	**3**
SHOC1	7924	29	0.58	**8**	34.6	**<0.0001**	70.37	**<0.0001**	47.82	**<0.0001**	**8**
RNF212	3074	29	0.52	**8**	12.59	**0**	17.74	**0**	17	**<0.0001**	**4**
MSH4	3167	28	0.2	**8**	21.49	**<0.0001**	57.91	**<0.0001**	22.88	**<0.0001**	**4**
MSH5	5681	29	0.24	**8**	0	1	13.65	**0**	25.4	**<0.0001**	0
F) Resolution											
HFM1/MER3	8134	29	0.37	**8**	0	1	58.64	**<0.0001**	41.93	**<0.0001**	**2**
CNTD1	3168	29	0.3	**8**	7.58	**0.02**	10.57	**0.01**	6.01	**0.01**	**1**
MLH1	6294	29	0.18	8a	0	1	16.21	**0**	1.78	0.18	0
MLH3	5051	29	0.44	**8**	33.41	**<0.0001**	70.92	**<0.0001**	40.57	**<0.0001**	**11**

Significant *P*-values and BEBs > 0 are bolded.

($P = 0.824$, Fisher's exact test) or number of genes returning potential sites ($P = 0.558$, Fisher's exact test). Because multinucleotide mutations (MNMs) can cause false positive signatures of selection (Venkat et al. 2018), we reanalyzed all genes for which Model 8 was the best fit after removing codons that HyPhy's FitMultiModel reported as potential MNM sites (Lucaci et al. 2021). After this removal, all genes retained their signatures of positive selection except *CNTD1*, *NBS* and *MSH5* (supplementary table S7, Supplementary Material online). To ensure consistency across clades, we performed the same MNM analysis on mammal recombination genes with signatures of positive selection from Dapper and Payseur (2019), with no significant difference in signal (supplementary table S8, Supplementary Material online).

We sought to identify the location of codons under positive selection in avian recombination genes to determine if they were in functionally important regions. Unfortunately, we were unable to find annotated domains for many of the codons. However, we were able to identify codons with signatures of positive selection within a GAR motif in *MRE11* (581), an N-terminal in *REC8* (51 to 53), within subunit A in *SPO11* (301, 306), and within a Tetratricopeptide-like helical repeat (TPR) in *TEX11* (492). The GAR motif in *MRE11* is associated with DSB repair and the recruitment of *RAD51* to damaged sites in mice (Yu et al. 2012b). Two codons in *SPO11* (sites 301 and 306) are located within a Toprim domain, associated with catalyzing double-stranded breaks (Zheng et al. 2025). The N-terminal in *REC8* is associated with binding to the ATPase heads of cohesin subunits *Smc3* and *Smc1* in mammalian cell lines. This complex is associated with the synapsis of sister chromatids (Xu et al. 2005; Zhang et al. 2013). TPRs are associated with protein–protein interactions, and the sites under positive selection within the TPR region in TEX11 could be associated with adherence to the MRN complex or synaptonemal complex binding (Adelman and Petrini 2008). While this is not an exhaustive analysis, there is evidence to suggest that proteins associated with the formation, processing, and resolution of double stranded breaks have undergone adaptive evolution, consistent with previous findings in mammals (Dapper and Payseur 2019).

To determine whether the elevated signatures of adaptive evolution we observed was specific to the recombination pathway, or a more general feature of the avian genome, we conducted the same set of analyses on two control panels of genes. First, we selected a conserved pathway involved with the Sonic Hedgehog (SHH) pathway of brain development (*BMI1, CCNA2, CCNB1, CCND1, CCND2, DHH, EN1, EN2, FOXM1, GLI1, GLI2, GLI3, IGF2, IHH, MYCN, PTCH1, SHH, SMO, SUFU;* Oliver et al. 2003; Vaillant and Monard 2009; Liu et al. 2014; Carballo et al. 2018). While we did observe evidence of positive selection in genes involved in this pathway across the avian phylogeny, the incidence was

Table 2 Comparison of means of recombination, brain, and up/downstream genes for birds, mammals, and teleost fish

	Birds		Mammals		Fish	
	Brain	Up/Downstream	Brain	Up/Downstream	Brain	Up/Downstream
Recombination	**0.02058**	**0**	**<0.0001**	**<0.0001**	**<0.0001**	**<0.0001**
Brain	…	0.6462	…	0.7125	…	0.1232

Bolded values are significant via ANOVA/Tukey HSD test, $\alpha = 0.05$.

Table 3 Genes with elevated (1 SD above the mean) and lower (1 SD below the mean) rates of molecular evolution by clade

Clade	Gene
Omega 1 SD above mean	
Mammal	IHO1
Bird	RNF212
Fish	IHO1
Omega 1 SD below mean	
Mammal	BRCC3
Bird	DMC1
Fish	RAD50

not significantly higher than that observed in mammals (Table 4, $P = 0.6052$, Fisher's exact test). Out of 19 genes, 3 (15.8%) showed evidence of positive selection in birds (Model 8): *FOXM1, GLI3,* and *SHH*. We see similar trends in mammals, identifying one gene with signatures of positive selection (*GLI2*, supplementary table S9, Supplementary Material online). As expected, there is a significant difference in the ratio of genes with signatures of positive selection between the SHH pathway and the avian meiotic recombination pathway ($P = 0.001$, Fisher's exact test).

The same pattern holds true for our second panel of control genes located directly up or downstream of recombination genes (supplementary table S10, Supplementary Material online). Of 33 genes in birds, 6 (20%) exhibited signatures of positive selection (*COA3, DECR1, EPB41L2, GPR83, KTN1,* and *MED23*, supplementary table S11, Supplementary Material online). This is a significantly lower incidence of signatures of positive selection compared to recombination genes ($P = 0.0002$, Fisher's exact test). We also identified significantly fewer signatures of positive selection within mammals, with only 2 of 32 (6.25%) genes containing these signatures: CBY1 and MED23 (supplementary table S12, Supplementary Material online; $P = 0.0109$, Fisher's exact test).

There is Little Evidence of Positive Selection in the Teleost Recombination Pathway

Consistent with their overall lower rate of molecular evolution, only two recombination pathway genes showed signatures of positive selection within teleost fish: *DMC1* and *RAD50* (supplementary table S5, Supplementary Material online). Despite these signatures of positive selection, there were no reported codon sites impacted by positive selection (BEB, $P >$ 95%) (supplementary table S5, Supplementary Material online). These signatures persist with the removal of possible multinucleotide mutation sites. Interestingly, both *DMC1* and *RAD50* are highly conserved despite maintaining signatures of positive selection ($\omega_{DMC1} = 0.0572$, $\omega_{RAD50} = 0.1101$), suggesting that these signatures of selection likely come from a small number of sites. Thus, the elevated levels of positive selection in the recombination pathway do not appear to be universal to all vertebrate clades. Additionally, there were very few signatures of positive selection in the other gene panels analyzed. Of the brain panel, only 1 of 16 (6.25%) of fish brain genes had signatures of positive selection (*CCND1*), though there were no specific sites identified (BEB, $P > 95\%$; supplementary table S13, Supplementary Material online). There were no signatures of positive selection found within the up/downstream genes in teleost fish (supplementary table S14, Supplementary Material online).

Signatures of Positive Selection Are not Concentrated in Specific Steps of the Avian Recombination Pathway

All genes that had signatures of positive selection in mammals also had signatures of positive selection in birds, resulting in a significant correlation between genes under positive selection between the two clades ($P = 0.0035$, Fisher's exact test). However, in contrast with the observation in mammals, we did not find that signatures of positive selection are concentrated in genes that regulate the CO/NCO decision in avian genomes (Table 5). This is due to the increased incidence of positive selection in other steps of the avian recombination pathway. We did observe a significant paucity of genes with signatures of positive selection in the steps of the pathway involved in DSB processing and homology search and strand invasion steps, consistent with strong purifying selection acting on the genes that identify and process DNA damage ($P = 0.0108$, Fisher's exact test, Table 5).

Integrating Polymorphism Data Reveals Signatures of Purifying Selection in the Avian Recombination Pathway

We leveraged polymorphism data within chickens, available for 17 of the recombination genes in our panel, and divergence between chickens and ducks to further explore signatures of selection on the recombination pathway across the avian clade (Yang et al. 2021). The McDonald-Kreitman Test compares rates of polymorphism with rates of divergence ($P_N P_S / D_N D_S$; Mcdonald and Kreitman 1991). When the null assumption is violated, the presence and direction of natural selection can be inferred. Purifying selection is inferred when $P_N P_S / D_N D_S > 1$, due to an over-representation of polymorphic alleles. Positive selection is inferred when $P_N P_S / D_N D_S < 1$, which occurs when there is less polymorphism in a population due to the fixation of advantageous alleles. We identified nine genes with significant McDonald–Kreitman tests, supported by neutrality indices (NI) and direction of selection (DoS) ($P < 0.05$, Fisher's exact test, Table 6). However, in all cases, the results were consistent with purifying, rather than positive, selection. The McDonald–Kreitman tests shown in Table 6 support the presence of purifying selection in several genes PAML identified as experiencing positive selection (*MRE11*, *SPATA22*, *MEIOB*, *SYCP1*, *HFM1*). There are a couple of reasons why this apparent discordance is not surprising. First, the McDonald–Kreitman test is conservative, requiring strong gene-wide signatures to produce

Table 4 Evolutionary rates and tests for positive selection across birds at 19 brain development genes, including likelihood ratio tests for each model, average omega across the gene, and number of codon sites potentially experiencing positive selection (BEB, $P > 95\%$)

Gene	bp	N	omega	M	M1-M2	P	M7-M8	P	M8a-M8	P	BEB
BMI1	3033	20	0.0205	7	0	1	0	0.9970	…	…	0
CCNA2	1917	27	0.1225	7	0	1	3.7940	0.1501	…	…	0
CCNB1	1500	13	0.1611	7	0	1	0	1	…	…	0
CCND1	4348	29	0.0341	7	0	1	0	0.9990	…	…	0
CCND2	5663	29	0.0666	7	0	1	0	1	…	…	0
DHH	3158	23	0.0693	7	0	1	0.9440	0.6238	…	…	0
EN1	2045	24	0.1204	7	0	1	0.4130	0.8135	…	…	0
EN2	2032	20	0.0490	7	0	1	0	1	…	…	0
FOXM1	3743	28	0.3612	**8**	14.7470	**0.0006**	37.7410	**<0.0001**	16.1950	**0.0001**	**1**
GLI1	4437	28	0.2122	7	0	1	2.5250	0.2830	…	…	0
GLI2	7564	28	0.1112	8a	0	1	7.5140	0.0234	0.8280	0.3628	0
GLI3	9272	29	0.1586	**8**	0	1	17.7500	**0.0001**	6.6620	**0.0099**	**6**
IGF2	5722	29	0.0697	7	0	1	0	1	…	…	0
IHH	2679	28	0.1094	7	0	1	3.9060	0.1418	…	…	0
MYCN	1326	28	0.1595	7	0.3060	0.8579	2.0750	0.3543	…	…	0
PTCH1	7679	27	0.1048	8a	0	1	12.5130	**0.0019**	1.0060	0.3159	0
SHH	1535	28	0.1490	**8**	13.8600	**0.0010**	20.5610	**<0.0001**	12.8200	**0.0003**	**5**
SMO	3257	27	0.1152	8a	5.5420	0.0626	11.9720	**0.0025**	2.1070	0.1466	0
SUFU	7842	29	0.0248	7	0	1	3.9840	0.1365	…	…	0

Significant *P*-values and BEBs > 0 are bolded.

Table 5 Comparison of proportion of genes with signatures of positive selection by recombination pathway step: (A) DSB formation, (B) DSB processing, (C) Homology search and strand invasion, (D) Synapsis, (E) CO/NCO decision, (F) Resolution

	Focal steps		Other steps		Fisher's exact test
Focal step(s)	Yes	No	Yes	No	*P*-value
A	4	1	15	9	0.6328
B	2	3	17	7	0.3064
C	**1**	**4**	**18**	**6**	**0.0357**
D	4	1	15	9	0.6328
E	5	0	14	10	0.1336
F	3	1	16	9	1
A,B	6	4	13	6	0.6981
B,C	**3**	**7**	**16**	**3**	**0.0108**
C,D	5	5	14	5	0.2439
D,E	9	1	10	9	0.0976
E,F	8	1	11	9	0.1071

Significant *P*-values, focal steps, and values are bolded.

significant results. However, in most cases, both positive and purifying selection are acting on the same gene at different sites which can lead to differing conclusions between PAML and the McDonald–Kreitman test (Pavlova et al. 2017; Bahbahani et al. 2023). The branch-site models used within PAML are used to detect signatures of positive selection on specific codons. Therefore, it is likely that positive selection is acting on specific sites in the midst of more conserved regions. Additionally, our results here are restricted to two branches within the avian phylogeny (chickens and ducks), while PAML considers molecular rates across all branches, increasing power to detect clade-wide signatures of positive selection.

Recombination Genes With Signatures of Positive Selection are Associated With Within-population, but not Interspecific, Variation in Recombination Rate

If the rapid evolution and signatures of positive selection observed among recombination genes are associated with their regulation of recombination rate, we may expect to see a correlation between rates of molecular evolution of genes and the overall rate of evolution of recombination rate. We used Coevol (Lartillot and Poujol 2010) to look for covariation between recombination rate and divergence of recombination genes. Within avians, we used the average number of *MLH1* foci and XO/HCN on chromosome 1 as an estimate of recombination rate. Because of the lack of available *MLH1* foci datasets in teleosts, we estimated XO/HCN from available map lengths. No avian genes showed a correlation between divergence and recombination rate (Table 7). However, as we were only able to include data from eight species in the avian analysis, our power to detect such correlations is low. Interestingly, we identified significant correlations between divergence in *RAD21L1* and *RNF212* in fish (Table 8). However, this significant correlation does not persist when controlling for variation in the rate of synonymous substitutions (dS).

We also predict that genes associated with within-population variation in recombination rate are more likely to contribute to between species divergence in recombination rate and exhibit signature of positive selection. While there are limited data on genes that are associated with within population variation in avian species, nine recombination genes included in our panel have been associated with variation in recombination rate in mammals: *REC114, REC8, RAD21L. RNF212, TEX11, MSH4, MSH5, HFM1*, and *MLH3* (Kong et al. 2008; Chowdhury et al. 2009; Sandor et al. 2012; Ma et al. 2015; Johnston et al. 2016; Kadri et al. 2016; Petit et al. 2017; Shen et al. 2018). Interestingly, all nine recombination genes associated with recombination rate variation in mammals have signatures of positive selection in birds. Compared to other genes in the pathway, recombination genes associated with variation in recombination rate in the mammalian clade are significantly more likely to have signatures of positive selection in the avian clade ($P = 0.0114$, Fisher's exact test). This is contrary to what we see in mammals, wherein genes associated with variation in mammalian recombination rate are not significantly more likely to experience signatures of positive selection compared with other meiotic recombination genes ($P = 0.2175$, Fisher's exact test).

Table 6 Comparisons of polymorphism within chickens to divergence between chicken and duck at recombination genes

	Pn	Ps	Pn/Ps	Dn	Ds	Dn/Ds	MK Test	alpha	NI	DoS	Direction
MEI4	26	8	3.25	81	48	1.6875	0.16	1.1368	1.9259	−0.14	…
REC114	6	2	3	53	43	1.2326	0.46	1.1979	2.4340	−0.2	…
IHO1	25	18	1.39	188	102	1.8431	0.4	0.9331	0.7535	0.07	…
MRE11	25	6	4.17	92	117	0.7863	**<0.001**	1.3663	5.2989	−0.37	Neg.
NBS1	69	35	1.97	174	133	1.3083	0.09	1.0967	1.5069	−0.1	…
RAD50	121	51	2.37	127	284	0.4472	**<0.001**	1.3945	5.3055	−0.39	Neg.
BRCC3	16	6	2.67	8	72	0.1111	**<0.001**	1.6273	24.0000	−0.63	Neg.
RAD51	12	3	4	8	85	0.0941	**<0.001**	1.7140	42.5000	−0.71	Neg.
SPATA22	15	2	7.5	78	63	1.2381	**0.01**	1.3292	6.0577	−0.33	Neg.
MEIOB	85	25	3.4	44	76	0.5789	**<0.001**	1.4061	5.8727	−0.41	Neg.
MCMDC2	58	18	3.22	61	141	0.4326	**<0.001**	1.4612	7.4481	−0.46	Neg.
RAD21L1	22	8	2.75	155	122	1.2705	0.08	1.1738	2.1645	−0.17	-
SYCP1	103	23	4.48	147	102	1.4412	**<0.001**	1.2271	3.1074	−0.23	Neg.
TEX12	1	0	-	69	18	3.8333	…	…	…	…	…
TEX11	26	9	2.89	202	51	3.9608	0.51	0.9444	0.7294	0.06	…
RNF212	11	3	3.67	15	12	1.2500	0.19	1.2302	2.9333	−0.23	…
HFM1	148	18	8.22	176	165	1.0667	**<0.001**	1.3754	7.7083	−0.38	Neg.

Significant *P*-values for the McDonald-Kreitman test are bolded.

Table 7 Correlations between substitution rate and recombination rate, measured as average *MLH1* foci across 8 species of birds for 29 recombination genes

	Correlation coefficient						Partial correlation coefficient					
Gene	dS - ω		dS – XO/HCN		ω – XO/HCN		dS – ω		dS – XO/HCN		ω – XO/HCN	
(A) DSB formation												
HORMAD1	−0.02	(0.49)	−0.034	(0.47)	−0.507	(0.21)	0.007	(0.50)	−0.039	(0.47)	−0.369	(0.26)
MEI4	0.251	(0.65)	**0.701**	**(0.96)**	0.247	(0.65)	0.170	(0.61)	0.424	(0.79)	0.107	(0.57)
REC114	0.004	(0.50)	0.202	(0.61)	0.259	(0.65)	0.004	(0.50)	0.149	(0.60)	0.189	(0.62)
IHO1	0.721	(0.91)	0.408	(0.85)	0.368	(0.78)	0.733	(0.91)	0.102	(0.57)	0.090	(0.55)
SPO11	−0.351	(0.29)	0.560	(0.91)	−0.308	(0.31)	−0.249	(0.34)	0.276	(0.70)	−0.176	(0.39)
(B) DSB processing												
HORMAD2	−0.063	(0.47)	0.198	(0.61)	0.052	(0.53)	−0.019	(0.49)	0.143	(0.59)	0.047	(0.53)
MRE11	0.142	(0.58)	0.410	(0.73)	0.364	(0.70)	0.050	(0.54)	0.265	(0.68)	0.267	(0.67)
NBS1	0.615	(0.85)	**0.805**	**(0.96)**	0.667	(0.88)	0.286	(0.70)	0.470	(0.81)	0.339	(0.72)
RAD50	−0.468	(0.22)	**0.800**	**(0.98)**	−0.287	(0.34)	−0.426	(0.22)	0.677	(0.92)	0.151	(0.60)
BRCC3	−0.038	(0.48)	0.472	(0.76)	−0.022	(0.49)	−0.015	(0.49)	0.301	(0.70)	−0.005	(0.50)
(C) Homology search and strand invasion												
DMC1	0.041	(0.48)	0.235	(0.63)	−0.058	(0.47)	−0.013	(0.49)	0.146	(0.60)	−0.041	(0.47)
RAD51	−0.294	(0.35)	**−0.915**	**(0.019)**	0.289	(0.65)	−0.131	(0.41)	−0.605	(0.12)	0.110	(0.58)
SPATA22	−0.51	(0.22)	0.759	(0.94)	−0.499	(0.23)	−0.225	(0.35)	0.450	(0.80)	−0.231	(0.34)
MEIOB	−0.17	(0.41)	0.192	(0.61)	−0.020	(0.49)	−0.068	(0.45)	0.122	(0.58)	0.012	(0.50)
MCMDC2	0.196	(0.62)	0.533	(0.92)	0.180	(0.61)	0.154	(0.59)	0.272	(0.71)	0.103	(0.56)
(D) Synapsis												
REC8	0.142	(0.59)	−0.021	(0.49)	−0.052	(0.44)	0.168	(0.60)	−0.015	(0.49)	−0.038	(0.47)
RAD21L1	0.342	(0.71)	0.015	(0.50)	0.100	(0.57)	0.413	(0.75)	−0.014	(0.49)	0.114	(0.57)
SYCP1	−0.107	(0.44)	−0.122	(0.38)	−0.218	(0.37)	−0.118	(0.43)	−0.092	(0.42)	−0.243	(0.35)
SYCP2	−0.119	(0.41)	0.249	(0.69)	−0.309	(0.31)	0.064	(0.54)	0.157	(0.61)	−0.298	(0.32)
TEX12	0.053	(0.53)	0.429	(0.81)	0.138	(0.58)	−0.001	(0.50)	0.253	(0.69)	0.115	(0.57)
(E) CO/NCO decision												
TEX11	0.092	(0.55)	0.161	(0.63)	−0.008	(0.50)	0.132	(0.58)	0.109	(0.58)	−0.022	(0.49)
SHOC1	−0.086	(0.44)	0.082	(0.59)	−0.004	(0.50)	−0.072	(0.46)	0.063	(0.55)	0.004	(0.50)
RNF212	−0.069	(0.46)	0.078	(0.54)	−0.233	(0.37)	−0.007	(0.49)	0.050	(0.53)	−0.165	(0.39)
MSH4	−0.055	(0.46)	0.318	(0.76)	0.075	(0.55)	−0.065	(0.45)	0.206	(0.66)	0.085	(0.55)
MSH5	−0.502	(0.20)	0.226	(0.63)	0.157	(0.58)	−0.484	(0.22)	0.153	(0.59)	0.284	(0.64)
(F) Resolution												
HFM1/MER3	0.211	(0.63)	−0.013	(0.48)	−0.029	(0.48)	0.233	(0.64)	0.013	(0.51)	−0.044	(0.47)
CNTD1	−0.082	(0.46)	0.219	(0.76)	−0.064	(0.47)	−0.021	(0.49)	0.326	(0.71)	−0.025	(0.48)
MLH1	0.129	(0.58)	0.289	(0.67)	0.294	(0.69)	0.094	(0.56)	0.217	(0.64)	0.188	(0.63)
MLH3	0.306	(0.69)	0.358	(0.84)	0.065	(0.56)	0.349	(0.71)	0.221	(0.68)	−0.061	(0.46)

Posterior probabilities are given in parenthesis. Significant correlations and posterior probabilities are bolded.

Discussion

Meiotic recombination is a near-ubiquitous biological process, necessary for the production of viable gametes. The rate at which recombination occurs within and between species shapes species divergence (Brooks and Marks 1986; Begun and Aquadro 1992; Lercher and Hurst 2002; Ptak et al. 2005; Kulathinal et al. 2008; Dumont et al. 2009; Nachman and Payseur 2012; Brand et al. 2018; Tigano et al. 2022). Importantly,

Table 8 Correlations between substitution rate and recombination rate, measured as XO/HCN across 13 species of fish for 28 recombination genes

	Correlation coefficient						Partial correlation coefficient					
Gene	dS – ω		dS – XO/HCN		ω – XO/HCN		dS – ω		dS – XO/HCN		ω – XO/HCN	
(A) DSB formation												
HORMAD1	0.253	(0.71)	0.142	(0.66)	0.155	(0.64)	0.292	(0.72)	0.114	(0.61)	0.111	(0.59)
MEI4	0.206	(0.64)	0.253	(0.79)	0.035	(0.53)	0.258	(0.68)	0.196	(0.67)	−0.032	(0.47)
REC114	0.013	(0.50)	0.517	(0.92)	−0.066	(0.46)	0.115	(0.58)	0.369	(0.78)	−0.119	(0.43)
IHO1	0.429	(0.78)	**0.584**	**(0.97)**	0.318	(0.73)	0.412	(0.76)	0.357	(0.77)	0.082	(0.55)
SPO11	−0.257	(0.27)	**0.552**	**(0.96)**	−0.354	(0.25)	0.017	(0.48)	0.483	(0.90)	−0.316	(0.30)
(B) DSB processing												
HORMAD2	0.100	(0.56)	0.424	(0.86)	−0.295	(0.25)	0.361	(0.76)	0.499	(0.87)	−0.400	(0.20)
MRE11	0.320	(0.73)	0.188	(0.72)	0.186	(0.64)	0.335	(0.73)	0.097	(0.59)	0.136	(0.59)
NBS1	−0.331	(0.23)	**0.506**	**(0.95)**	−0.254	(0.30)	−0.219	(0.35)	0.441	(0.89)	−0.117	(0.42)
RAD50	−0.199	(0.27)	0.419	(0.93)	0.128	(0.64)	−0.277	(0.20)	**0.472**	**(0.96)**	0.235	(0.75)
BRCC3	−0.037	(0.46)	**0.793**	**(0.99)**	−0.137	(0.35)	0.230	(0.65)	**0.825**	**(0.99)**	−0.291	(0.29)
(C) Homology search and strand invasion												
DMC1	0.766	(0.92)	**0.457**	**(0.96)**	0.482	(0.91)	0.758	(0.91)	−0.033	(0.48)	0.221	(0.64)
RAD51	0.060	(0.54)	0.094	(0.57)	0.043	(0.53)	0.075	(0.54)	0.058	(0.54)	0.030	(0.52)
SPATA22	−0.339	(0.27)	**0.622**	**(0.99)**	−0.322	(0.28)	−0.195	(0.37)	0.401	(0.81)	−0.204	(0.37)
MEIOB	0.407	(0.81)	0.310	(0.84)	0.672	(0.92)	0.337	(0.72)	−0.037	(0.48)	0.632	(0.87)
MCMDC2	−0.044	(0.44)	**0.505**	**(0.97)**	−0.379	(0.25)	0.288	(0.70)	0.455	(0.87)	−0.472	(0.19)
(D) Synapsis												
REC8	0.177	(0.63)	−0.187	(0.30)	−0.471	(0.19)	0.191	(0.63)	0.014	(0.49)	−0.489	(0.19)
RAD21L	0.782	(0.99)	0.514	(0.94)	**0.725**	**(0.97)**	**0.777**	**(0.96)**	−0.168	(0.38)	0.479	(0.79)
SYCP1	−0.361	(0.21)	0.169	(0.69)	0.372	(0.79)	−0.464	(0.18)	0.473	(0.91)	0.504	(0.84)
SYCP2	0.177	(0.63)	0.328	(0.84)	0.332	(0.79)	0.132	(0.58)	0.249	(0.76)	0.288	(0.74)
(E) CO/NCO decision												
TEX11	0.435	(0.87)	0.519	(0.94)	0.082	(0.59)	0.521	(0.90)	0.558	(0.94)	−0.243	(0.32)
SHOC1	0.563	(0.89)	0.404	(0.87)	0.051	(0.58)	0.650	(0.91)	0.476	(0.84)	−0.314	(0.28)
RNF212	0.689	(0.92)	**0.731**	**(0.95)**	**0.689**	**(0.95)**	0.477	(0.81)	0.365	(0.73)	0.274	(0.69)
MSH4	0.124	(0.58)	0.308	(0.85)	−0.081	(0.45)	0.191	(0.64)	0.273	(0.77)	−0.148	(0.39)
MSH5	−0.322	(0.23)	0.401	(0.91)	−0.493	(0.18)	−0.129	(0.41)	0.210	(0.69)	−0.461	(0.20)
(F) Resolution												
HFM1/MER3	0.155	(0.60)	0.461	(0.94)	−0.377	(0.22)	0.503	(0.85)	0.565	(0.93)	−0.571	(0.12)
CNTD1	0.229	(0.63)	0.411	(0.94)	−0.003	(0.52)	0.285	(0.66)	0.279	(0.72)	−0.167	(0.39)
MLH1	−0.371	(0.24)	**0.578**	**(0.97)**	−0.201	(0.36)	−0.337	(0.27)	0.422	(0.83)	−0.006	(0.51)
MLH3	−0.334	(0.24)	0.413	(0.91)	−0.315	(0.30)	−0.200	(0.36)	0.259	(0.76)	−0.258	(0.35)

Posterior probabilities are given in parenthesis. Significant correlation coefficients and posterior probabilities are bolded.

recombination rate itself evolves and exhibits striking patterns of divergence between populations, even over relatively short time scales (Kong et al. 2008; Dumont et al. 2009; Sandor et al. 2012; Johnston et al. 2016, 2018; Kadri et al. 2016; Petit et al. 2017). Recombination events arise through a highly regulated cellular pathway (Keeney 2001; Youds and Boulton 2011; Baudat et al. 2013; Cannavo et al. 2020), indicating that molecular changes in the underlying genes shape the phenotypic evolution of this fundamental genomic parameter, motivating a comparative study of the molecular evolution of the genes that regulate this pathway.

Recombination Rates are More Variable Across Avian and Teleost Clades

If recurrent adaptive evolution contributes to divergence in recombination rate, we may expect to observe more signatures of positive selection in clades with higher rates of phenotypic evolution. Although differences in genome architecture make it difficult to disentangle the contribution of karyotypic evolution and molecular evolution to divergence in recombination rate, we leveraged existing *MLH1* foci and linkage map data to compare recombination rates between avian, teleost, and mammalian genomes. We found that the number of crossovers (*MLH1* foci) on chromosome 1, by convention the largest chromosome in the genome, is higher and more variable in avian genomes than in mammals. Importantly, divergence in foci number is not explained by differences in chromosome size but is positively correlated with the length of the synaptonemal complex (SC), the proteinaceous structure that stabilizes the pairing of homologous chromosomes and provides a substrate for the resolution of crossovers, which is longer relative to chromosome size in avian genomes than in mammalian genomes (von Wettstein et al. 1984). Thus, these differences are likely driven by molecular changes in the recombination pathway, rather than as a direct result of changes to the size and structure of chromosomes in the avian genomes. However, the evolution of microchromosomes in avian genomes may have indirectly generated selection for higher recombination rates in avian genomes to ensure the minimum of one crossover per chromosome necessary for proper chromosomal segregation (Hassold and Hunt 2001; Ellegren 2010). Interestingly, our meta-analysis reveals that fish have very similar patterns of variation in recombination rate to birds, despite largely lacking microchromosomes. In fact, there are no significant differences in the rate of recombination between focal bird and teleost species. Due to the lack of *MLH1* data in fish, we do not know if teleost genomes exhibit the degree of variation in crossovers per chromosome that we observed in avian genomes.

The Rapidly Evolving Meiotic Recombination Pathway Experiences Similar Selective Pressures Across Vertebrate Clades

Consistent with prior observations in mammals (Dapper and Payseur 2019), recombination genes have significantly

elevated rates of molecular evolution in both avian and teleost clades. While the overall rate of evolution of recombination genes was lower in teleosts than birds or mammals, we also observed lower rates of evolution in both control panels in this clade. Thus, the lower rates of evolution are likely due to genome-wide factors, like higher effective population size. Thus, despite substantial differences between these clades, there is a general pattern of rapid evolution within the meiotic recombination pathway. Importantly, elevated rates of molecular evolution are frequently observed in reproductive genes (Civetta and Singh 1999; Singh and Kulathinal 2000; Swanson and Vacquier 2002; Oliver et al. 2009) and can result from either positive selection or relaxed purifying selection (Dapper and Wade 2016, 2020). However, the factors generally hypothesized to produce these patterns do not appear to apply here. The recombination genes we analyzed are not sex-specific, which is expected to relax selection, nor are they likely to be involved in post-copulatory sexual selection.

In addition to overall higher rates of molecular evolution, we also identified a high correlation between rates of molecular evolution of recombination pathway genes across clades. This result suggests that the evolutionary pressures (i.e. selection, drift, and mutation) that shape recombination rate are largely consistent across vertebrates.

TEX11 May be a Driver of Mammalian Meiotic Recombination Evolution

Within our panel of key recombination genes, we identified one notable outlier, *TEX11*, in the comparison of evolutionary rates between clades. While *TEX11* evolves very rapidly in mammals (Dapper and Payseur 2019), its evolutionary rate across birds and teleost fish is considerably slower and on par with the average rate of evolution of the recombination pathway in these clades. *TEX11* is particularly interesting because it plays a crucial role in crossover formation and synapsis maintenance (Yang et al. 2008) and its evolutionary rate is correlated with genome-wide recombination rate across mammals (Dapper and Payseur 2019).

Notably, all studies of *TEX11* phenotype are from mammalian systems (Yang et al. 2008, 2015; Tang et al. 2011; Yu et al. 2012a, 2021; Yatsenko et al. 2015; Ji et al. 2021; Kitayama et al. 2022; Song et al. 2023). Together, these observations suggest that TEX11 may be a mammal-specific driver of recombination rate variation. Thus, despite the overall concordance between evolutionary patterns, clade-specific drivers of the evolution of recombination rate may play important roles in driving divergence.

Signatures of Positive Selection are Significantly Elevated in Birds

Signatures of positive selection in recombination genes provide support for the prediction that directional selection is a driver of molecular evolution of recombination rate (Segura et al. 2013). In order to determine if there is more evidence of positive selection in non-mammal recombination pathway genes, we performed rigorous comparative phylogenetics, using PAML to identify signatures of positive selection at the codon level. We observed a striking elevation in the signatures of positive selection among genes in the recombination pathway across the avian phylogeny, with 19 out of 29 genes surveyed exhibiting significant signatures of selection. This is significantly higher than the 11 out of 32 genes identified with signatures of positive selection in the mammalian recombination pathway (Dapper and Payseur 2019) and the 2 of 28 identified in teleosts. To account for the possibility of poorer genome quality, we excluded available genome assemblies with significant issues in gene alignment prior to data collection and analysis. As maximum likelihood models are prone to false positives, we took a number of steps to verify these results, including hand-curation to minimize misalignment, utilization of models that account for multi-nucleotide mutations (Venkat et al. 2018; Lucaci et al. 2021), and reanalysis of the mammalian data to ensure consistency in data preparation and analysis. While in a few cases these measures removed signals of positive selection, there was no meaningful change to the overall result. We also selected two control pathways not involved in meiotic recombination, or reproductive processes, which we analyzed using the same pipeline. Our control pathways did not exhibit patterns of rapid evolution, such as that observed in some recombination genes, nor did we observe a significant elevation in incidence of positive selection. Thus, our result is unlikely to be the result of lower overall genome quality among the included avian species.

Such elevated signatures of positive selection in avians further support the possibility of clade-specific drivers of recombination rate evolution. While recombination genes are evolving rapidly in all clades, it is possible that the differences in signatures of selection within these genes are due to avian-specific genome structure. Avian genomes have a different size and structure than either mammalian or teleost genomes: they contain microchromosomes (Waters et al. 2021). If microchromosomes in avian genomes experienced selection for higher recombination rates to meet the one-crossover rule, perhaps by selecting for longer synaptonemal complexes, this shift in genome architecture could drive recurrent positive selection on the recombination pathway across the avian phylogeny (Hassold and Hunt 2001; Ellegren 2010).

In contrast with birds and mammals, there are very few signatures of positive selection in teleost fish recombination genes. The relative paucity of signatures of selection may be the result of lower power to detect patterns of positive selection due to overall stronger purifying selection in this clade—or because the recombination pathway has not experienced the same degree of recurrent positive selection in fish genomes. Interestingly, the teleost genomes have experienced a more recent whole genome duplication event than avian and mammalian clades (Taylor et al. 2003). Such events are expected to exert strong selection on the recombination pathway because tetraploidy can increase instances of aneuploidy during meiosis (Comai 2005; Bomblies et al. 2016; Paim and FitzHarris 2019). Notably, of the two teleost recombination genes with signatures of positive selection, one (*RAD50*) is part of the complex that processes new DSBs, holding broken ends of DNA together, where the other (*DMC1*) helps catalyze homologous chromosome pairing (Tarsounas et al. 1999; Lamarche et al. 2010). While only two teleost recombination genes exhibited signatures of positive selection, there is considerable overlap in the most and least rapidly evolving recombination genes among clades. These repeated patterns of positive and purifying selection within recombination pathway genes between clades suggest that while there are significant phenotypic differences between clades, there are predictable effects of selection acting on the meiotic recombination pathway.

Predictable Selection Pressures Govern Pathway Step Evolution

The structure of the recombination pathway suggests that divergence in rate may arise from upstream changes that alter

the number of potential crossover sites (DSB formation) and/or downstream changes that regulate the number of potential sites that are resolved as mature crossovers (CO/NCO decision; Martini et al. 2006; Cole et al. 2012; Sandor et al. 2012; Kadri et al. 2016; Ortiz-Barrientos et al. 2016; Petit et al. 2017; Johnston et al. 2018). Molecular genetic and evolutionary analyses in mammals suggest that protein-coding and/or regulatory changes to genes that regulate the crossover (CO) versus noncrossover (NCO) decision are most likely to affect the evolution of recombination rate (de Vries et al. 1999; Romanienko and Camerini-Otero 2000; Yang et al. 2008; Dumont et al. 2009; Kumar et al. 2010; Reynolds et al. 2013; Segura et al. 2013; Kadri et al. 2016; Guiraldelli et al. 2018; Dapper and Payseur 2019). However, as a result of the high incidence of signatures of positive selection across the avian meiotic recombination pathway, genes experiencing signatures of positive selection are not concentrated in the CO/NCO decision pathway steps, as seen in mammals. Instead, there are significant signatures of positive selection within the steps of the pathway responsible for the formation of double-stranded breaks, synapsis, and the CO/NCO decision. This supports the hypothesis that changes in proteins that govern SC development and maintenance within the avian genome may contribute to differences in recombination rate between mammals and birds but also raises the prospect that variation may also be driven by differences in the number of double-strand breaks generated early in the pathway. Conversely, there is evidence of significant purifying selection acting on avian recombination genes that process and identify DNA damage, a trend also seen within mammals.

One limiting factor of our detection of signatures of positive or purifying selection along the phylogeny lies with the McDonald–Kreitman (MK) test, which can return underestimated rates of positive selection in the presence of sightly deleterious mutations and variable site effective population sizes (Fay et al. 2001; Charlesworth and Eyre-Walker 2008; Eyre-Walker and Keightley 2009). The lack of available polymorphism data for all species examined in this study also limits our ability to use the MK test detect adaptive evolution along the phylogeny. Notably, the polymorphism data in our study comes from two closely related taxa (duck and chicken). It is possible that with more phylogenetically diverse data, the preponderance of slightly deleterious mutations in polymorphism datasets would not have such a strong masking effect on signatures of positive selection.

Genes Associated With Intra-specific Variation are More Likely to Exhibit Signatures of Positive Selection

Importantly, while patterns of molecular evolution can be indicative of recurrent positive selection acting on protein-coding genes, they do not reveal the source of the selective pressure. Thus, while our observation of elevated signatures of positive selection is consistent with the hypothesis that selection favored elevated rates of recombination across the avian phylogeny, it is also possible that these signatures arise as result of pleiotropic selection. If the molecular evolution of these genes is driven by their effect on recombination rate, we may expect to observe the following: (i) correlations between the rates of phenotypic and molecular evolution, such as the positive correlation between the rate of molecular evolution in *TEX11* and recombination rate across the mammalian phylogeny Dapper and Payseur (2019) and (ii) genes in the recombination pathway that influence recombination rate are more likely to exhibit signatures of positive selection than those that do not.

In contrast to our first prediction, we did not observe a significant correlation between evolutionary rate and recombination rate across the avian or teleost phylogenies. However, it is important to note because we were only able to include eight species in this analysis, we have limited power to detect such a correlation. This lack of correlation may also be consistent with a realistic scenario in which the interplay between genetic drift and purifying selection shape the overall rate of evolution of genes, and positive selection acted on small subset of impactful sites.

Previous studies identified recombination gene variants associated with recombination rate variation within mammals. If genes implicated in mammalian recombination rate variation behave similarly in avians and teleosts, we would expect to see high correlation between these and genes with signatures of positive selection. Interestingly, in line with our second prediction, we did observe a significant positive correlation between genes associated with within-population variation in recombination rate in mammalian populations and thus likely to impact recombination rate in avian genomes, and those that exhibited a significant signature of positive selection across the avian phylogeny. Given the overall conservation of function of genes in the recombination pathway, this correlation suggests that molecular evolution of these genes across the avian phylogeny may contribute to variation in recombination rate. We did not find a significant correlation between genes associated with mammalian variation in recombination rate and genes that exhibit signatures of positive selection in mammals. However, the overall lower number of genes experiencing positive selection in mammals may reduce our power to identify such a correlation, as there is also a significant correlation between the genes experiencing positive selection in avian and mammalian genomes. All genes that had signatures of positive selection in mammals also had signatures of positive selection in birds, providing additional support for the hypothesis that positive selection may act on the meiotic recombination pathway in predictable ways.

One important caveat to our study is the potential confounding effect of GC-biased gene conversion (gBGC) on signatures of positive selection reported by PAML. This process may result in mildly deleterious G/C alleles being favored over neutral A/T alleles, artificially inflating the dN/dS ratio of the region (Galtier and Duret 2007; Ratnakumar et al. 2010). There is also some evidence to suggest that gBGC can have a significant impact on measures of dN/dS in Ficedula flycatchers and Galloanserae (Bolívar et al. 2016; Rousselle et al. 2019). Despite the risk of false positives within PAML's measures of selection, we still see patterns of non-synonymous changes in recombination genes in birds, coupled with phenotypic changes in recombination rate, linking changes in genes regulating meiotic recombination mechanisms to phenotypic divergence.

Understanding the impact of changes to proteins involved in meiotic recombination is crucial to elucidating mechanisms responsible for between-species divergence. This study substantiates the existence of similar selective landscapes acting upon the meiotic recombination pathway between vertebrate clades. Specifically, we identify strikingly similar rates of molecular evolution within key avian, teleost and mammalian recombination genes. TEX11, an important element of the CO/NCO decision, is a significant outlier to this trend, suggesting the possibility of clade-specific drivers of meiotic

recombination rate variation. Additionally, we identify strong between-clade patterns of selection acting on recombination pathway genes: Patterns of positive selection acting on genes mediating recombination rate variation and those responsible for the formation and resolution of double-stranded breaks, and patterns of purifying selection acting upon genes responsible for DNA damage identification and processing, suggesting that changes in recombination pathway proteins drive recombination rate variation.

Methods

Meta-Analysis of Cytological Data

We collected data from published cytological studies of avian ($N = 9$, male; $N = 14$, female) and mammalian ($N = 11$, male) genomes (supplementary file S1, Supplementary Material online). All studies included in the meta-analysis used immunofluorescence to label *MLH1* foci, with two exceptions which used phosphotungstic acid. Due to difference in the feasibility of gamete collection, the mammalian studies almost exclusively report *MLH1* data from male sperm cells, while the majority of avian studies report *MLH1* data from female egg cells. As we did not observe significant heterochiasmy in avian genomes ($P = 0.4764$, *t*-test, supplementary fig. S1, Supplementary Material online), we report data that maximized sample size by comparing male and female avian *MLH1* estimates and male mammalian *MLH1* estimates. Analyses that included only male estimates supported the same conclusions and can be found in the supplementary material (supplementary fig. S2, Supplementary Material online). In cases where multiple MLH1 foci counts were reported for a single species, we chose to include data from the study with the largest sample size (determined by the number of individuals and total cell count). All included studies reported the average genome-wide *MLH1* foci count (a proxy for the total number of crossovers in the genome). We compared two measures of genome-wide recombination rate: (i) total number of MLH1 foci per haploid chromosome number (XO/HCN) and (ii) estimated centimorgans per megabase (cM/Mb). To estimate genetic map length from *MLH1* foci data, we multiplied the number of *MLH1* foci by 50 cM/foci, giving us an estimate of genetic map length (cM). We then divided total map length by genome size measured in Mb. We estimated genome size using two approaches: (i) by using the total size of the genome assembly (Mb), which may underestimate length because they may not include regions of the genome that are difficult to assemble and (ii) by converting genome weight (C-value, pg) to an estimated genome size (Mb). Genome weights were found using the Animal Genome Size Database (Gregory 2024). For the conversions, we assumed that 1 pg is roughly 978 Mb (Gregory 2024). Both methods of estimating total genome size produced qualitatively similar results (supplementary file S1, Supplementary Material online).

All avian studies and a subset of mammalian studies ($N = 8$, mammals) reported the average number of *MLH1* foci counts for the largest chromosome in the genome (by convention chromosome 1). To test whether variation in number of *MLH1* foci on Chromosome 1 could be explained by variation in chromosome size, we used the size of Chromosome 1 (Mb) as reported in the latest genome assembly of each species. Many of the cytological studies we surveyed also reported estimated length of the synaptonemal complex on Chromosome 1 ($N = 9$, male, mammal; $N = 6$, male, avian; $N = 7$, female, avian). All analyses were performed using R Statistical Software [v4.3.0; R Core Team 2021 R Core Team (2023)].

Because we used linkage map data in fish, as opposed to *MLH1* foci data, we took a different approach to estimating recombination rates. We estimated teleost fish recombination rates as cM/Mb by dividing previously published map lengths (cM) by the length of the assembly (Mb). Assemblies used may be found in supplementary table S4, Supplementary Material online, and data may be found in supplementary file S1, Supplementary Material online. In order to estimate teleost recombination rates as XO/HCN, we first divided the linkage map by 50. This is because one centimorgan is equivalent to a 1% chance of a recombination event. However, the greatest recombination frequency one can identify is 50% due to the independent assortment of alleles during meiosis. Dividing the map length by 50 cM allows us to estimate average number of crossover events during meiosis, independent of linkage between alleles or crossover interference (Chuang and Smith 2023; Kivikoski et al. 2023). Once we had an average number of crossovers per meiosis, we divided the crossover number by the haploid chromosome number for each species.

Data Acquisition and Processing

We utilized the same panel of 32 genes from Dapper and Payseur (2019) to compare meiotic recombination rate pathway evolution between mammals, birds, and teleosts (supplementary table S1, Supplementary Material online). Reference sequences were downloaded from NCBI from 29 bird species and 24 teleost fish species (Fig. 3). These species were chosen due to their divergence times and quality of reference sequences. However, we were unable to identify orthologs of all 32 recombination genes in avian and teleost genomes. Thus, 29 candidate genes were investigated in birds (supplementary table S1, Supplementary Material online). *RNF212B, HEI10,* and *MUS81* were excluded entirely from both birds and teleosts due to a lack of useful data. *TEX12* was not available for teleost fish, so we excluded this gene during analysis, resulting in 28 focal genes for the teleost recombination pathway. Phylogenetic trees were inferred using TimeTree, which allows the generation of trees from species lists, and fasttree, which allows high-throughput tree generation (Price et al. 2010; Kumar et al. 2022). We then generated visual trees with iTOL v.5 (Letunic and Bork 2021). For 26 genes, sequences were available from all species of birds. Sequences were not available for one or more individuals for the following genes: *MRE11, SYCP1,* and *MSH4*. Sequence availability proved more difficult in teleost fish. Data were unavailable for one or more teleost fish for 11 genes; however, all genes surveyed had at least 18 teleost species represented.

To control for differences in genome quality between clades in our subsequent analyses, we also selected a focal panel of control genes involved in a brain development pathway (*BMI1, CCNA2, CCNB1, CCND1, CCND2, DHH, EN1, FOXM1, GLI1, GLI2, GLI3, IGF2, IHH, MYCN, PTCH1, SHH, SMO, SUFU*; Oliver et al. 2003; Vaillant and Monard 2009; Liu et al. 2014; Carballo et al. 2018). We selected these genes for their inclusion in a well-described pathway and because we expect them to be conserved.

While dN/dS is a helpful metric for determining rates of molecular evolution, it is difficult to directly compare clades with significantly different effective population sizes. In order to determine if omega values differ due to selective pressures or

historical effective population size, we selected a panel of 33 genes found up- or down-stream of chicken recombination genes (supplementary table S10, Supplementary Material online). We identified orthologs of these genes between our focal mammal, bird, and fish species. We used this panel to determine if rates of molecular evolution differed significantly both between clades and between gene panels.

Phylogenetic Comparative Approach

We used maximum likelihood approaches to assay evidence of selection [using the same approach as (Dapper and Payseur 2019)]. We used CODEML site models from PAML to measure the rate of synonymous to non-synonymous substitutions (Miyata and Yasunaga 1980; Yang 2007). CODEML requires a phylogenetic tree, for which we used Newick format, and multiple sequence alignments, for which we used PHYLIP format (Felsenstein 2005). To ensure high quality files for analysis, we aligned reference sequences acquired from NCBI using MUSCLE and GBlocks via TranslatorX and AliView (Castresana 2000; Edgar 2004; Abascal et al. 2010; Larsson 2014), hand-cleaning when necessary. We aligned bird sequences with their mammalian counterparts to ensure that equivalent regions of the genes were compared. Specific assemblies used may be found in supplementary tables S2 and S4, Supplementary Material online. We used the JC69 model of codon substitution and set the following initial parameters: kappa = 2, omega = 0.4, alpha = 0. Rates were allowed to vary between branches (clock = 0). We calculated these rates for six site models (M0, M1a, M2a, M7, M8, M8a) and determined the model of best fit via likelihood ratio test. These procedures were followed for focal recombination genes, brain development genes, and a panel of genes found up- or down-stream of chicken recombination genes.

Identifying Signatures of Selection

A common method used to identify signatures of selection is comparing the ratio of synonymous (dS) to nonsynonymous substitutions (dN) (Anisimova et al. 2001). This is represented by $\omega = dN/dS$. If there are a larger number of non-synonymous amino acid changes than synonymous changes (higher dN), ω increases. If ω is significantly greater than 1, there is evidence of adaptive evolution. An ω value significantly less than 1 is indicative of purifying selection. Neutrally evolving sites will have an ω value close to 1. PAML's CODEML utilizes several evolutionary models to calculate the best fit for the data.

To determine model of best fit for bird recombination genes, we first compared Model 1 versus Model 2. M1 assumes that there are two classes of sites: one where $\omega < 1$, and one where $\omega = 1$, indicating neutral evolution. M2 introduces a third class, wherein $\omega > 1$, which indicates positive selection. Models 7 and 8 control for variation in ω across a beta distribution of 0 to 1. M7 contains 10 of these site classes where $\omega < 1$, whereas M8 includes a class of $\omega > 1$ to allow for positive selection. We compared M7, M8, and an additional model designated M8a. M8a allows $\omega = 1$. This model is frequently a better fit in genes where there are many sites that are evolving neutrally. We also report the number of codons undergoing positive selection (Bayes empirical Bayes, BEB; $P > 0.95$).

Multi-Nucleotide Mutations

Multinucleotide mutations (MNMs) occur when two or more mutations in proximity on one haplotype occur during the same mutational event (Wang et al. 2020). These mutations violate the assumptions of many maximum likelihood models of molecular evolution and can potentially contribute to false inferences of positive selection (Yang 2007; Venkat et al. 2018). In order to identify potential MNMs in our dataset, we used the FitMultiModelHyPhy analysis file to identify sites where a simultaneous nucleotide substitution model may fit better (Lucaci et al. 2021). We removed these sites and re-ran CODEML on the edited sequences. This process was done only for genes that showed evidence of positive selection to determine whether this signal remained after the removal of potential MNMs.

Polymorphism and Divergence

Polymorphism data were acquired from whole genome sequences of Nandao chickens (Yang et al. 2021). The data are available through the European Variant Archive, under the study identifier PRJEB46210. We used the asymptotic McDonald–Kreitman test due to its handling of small sample sizes and potential linkage between advantageous and mildly deleterious polymorphisms with Jukes–Cantor correction to compare synonymous and nonsynonymous substitutions and polymorphisms (Jukes and Cantor 1969; McDonald and Kreitman 1991; Haller and Messer 2017). Briefly, we downloaded chicken polymorphism data from PRJEB46210 and selected variants located within our genes of interest. We retrieved divergence data from comparing chicken and mallard sequences from the NCBI gene browser. Polymorphism and divergence data were compared using the web-based tool asymptoticMK (Haller and Messer 2017). At the time of the test, the web server was still available. However, the R code used to implement the test is still available at https://github.com/MesserLab/asymptoticMK. We also measured the neutrality index (NI), which measures divergence from the neutral expectation ($P_N/P_S = D_N/D_S$), and the direction of selection $(D_N/(D_N + D_S) - P_N/(P_N + P_S)$ for each gene (Stoletzki and Eyre-Walker 2011).

Evolutionary Rate Covariance

We used Coevol to identify any correlations between recombination rate and divergence of recombination genes between species. Briefly, Coevol uses Bayesian Markov Chain Monte Carlo (MCMC) methods to estimate correlations between traits and substitution rates in sequences given a phylogenetic tree (Lartillot and Poujol 2010). Instead of linkage map lengths, we used the number of MLH1 foci on chromosome 1 for eight species from our focal avian species list (*C. japonica*, *T. guttata*, *H. rustica*, *G. gallus*, *A. platyrhynchos*, *N. meleagris*, *M. alba*, and *M. gallopavo*) as a stand-in for recombination rate. We used the same parameters as Dapper and Payseur (2019) in Coevol (burn-in = 1,000; MCMC chain = 25,000; relative difference $\omega < 0.01$), which returned pairwise correlation coefficients between recombination rate, ω, and dS, along with partial correlation coefficients for each pairwise correlation (Dapper and Payseur 2019). We also investigated correlations between divergence and recombination rate measured as XO/HCN within the same focal bird panel, excluding M. alba, and in 13 species from our teleost fish phylogeny (*E. lucius*, *O. mykiss*, *S. salar*, *T. rubripes*, *C. semilaevis*, *H. burtoni*, *O. melastigma*, *G. morhua*, *I. punctatus*, *A. mexicanus*, *D. rerio*, *C. harengus*, and *S. formosus*).

Supplementary Material

Supplementary material is available at *Molecular Biology and Evolution* online.

Acknowledgments

We thank Austin Drury, Jean-Francois Gout, Federico Hoffmann, Mark Welch, and members of the Dapper and Gout labs for constructive feedback on study design and interpretation of results. This work was supported by National Science Foundation CAREER 2143063 to A.L.D.

Author Contributions

T.S.-G. lead data collection, data analysis, and writing. T.S.-G. and A.L.D. collaborated on study design, data analysis, and writing. K.S., V.V., and L.Z. contributed to data collection and analysis. A.K.L. assisted with identification of the control pathway.

Conflict of Interest

The authors declare no conflicts of interest.

Data Availability

Raw data may be found in the following repository: https://github.com/tszaszgreen/Meiotic_Recombination.

References

Abascal F, Zardoya R, Telford MJ. Translatorx: multiple alignment of nucleotide sequences guided by amino acid translations. *Nucleic Acids Res*. 2010:38(Web Server issue):W7–13. https://doi.org/10.1093/nar/gkq291.

Adelman CA, Petrini JHJ. ZIP4H (TEX11) deficiency in the mouse impairs meiotic double strand break repair and the regulation of crossing over. *PLoS Genet*. 2008:4(3):e1000042. https://doi.org/10.1371/journal.pgen.1000042.

Anderson LK, Reeves A, Webb LM, Ashley T. Distribution of crossing over on mouse synaptonemal complexes using immunofluorescent localization of MLH1 protein. *Genetics*. 1999:151(4):1569–1579. https://doi.org/10.1093/genetics/151.4.1569.

Anisimova M, Bielawski JP, Yang Z. Accuracy and power of the likelihood ratio test in detecting adaptive molecular evolution. *Mol Biol Evol*. 2001:18(8):1585–1592. https://doi.org/10.1093/oxfordjournals.molbev.a003945.

Auton A, Li YR, Kidd J, Oliveira K, Nadel J, Holloway JK, Hayward JJ, Cohen PE, Greally JM, Wang J, *et al*. Genetic recombination is targeted towards gene promoter regions in dogs. *PLoS Genet*. 2013:9(12):e1003984. https://doi.org/10.1371/journal.pgen.1003984.

Bahbahani H, Al-Zoubi S, Ali F, Afana A, Dashti M, Al-Ateeqi A, Wragg D, Al-Bustan S, Almathen F. Signatures of purifying selection and site-specific positive selection on the mitochondrial DNA of dromedary camels (*Camelus dromedarius*). *Mitochondrion*. 2023:69:36–42. https://doi.org/10.1016/j.mito.2023.01.004.

Baker BS, Carpenter ATC, Esposito MS, Esposito RE, Sandler L. The genetic control of meiosis. *Annu Rev Genet*. 1976:10:53–134. https://doi.org/10.1146/annurev.ge.10.120176.000413.

Baker SM, Plug AW, Prolla TA, Bronner CE, Harris AC, Yao X, Christie DM, Monell C, Arnheim N, Bradley A, *et al*. Involvement of mouse Mlh1 in DNA mismatch repair and meiotic crossing over. *Nat Genet*. 1996:13(3):336–342. https://doi.org/10.1038/ng0796-336.

Baker Z, Schumer M, Haba Y, Bashkirova L, Holland C, Rosenthal GG, Przeworski M. Repeated losses of PRDM9-directed recombination despite the conservation of PRDM9 across vertebrates. *eLife*. 2017:6:e24133. https://doi.org/10.7554/eLife.24133.

Baudat F, Buard J, Grey C, Fledel-Alon A, Ober C, Przeworski M, Coop G, de Massy B. PRDM9 is a major determinant of meiotic recombination hotspots in humans and mice. *Science (New York, N.Y.)*. 2010:327(5967):836–840. https://doi.org/10.1126/science.1183439.

Baudat F, Imai Y, de Massy B. Meiotic recombination in mammals: localization and regulation. *Nat Rev Genet*. 2013:14(11):794–806. https://doi.org/10.1038/nrg3573.

Begun DJ, Aquadro CF. Levels of naturally occurring DNA polymorphism correlate with recombination rates in *D. melanogaster*. *Nature*. 1992:356(6369):519–520. https://doi.org/10.1038/356519a0.

Bergerat A, de Massy B, Gadelle D, Varoutas P-C, Nicolas A, Forterre P. An atypical topoisomerase II from archaea with implications for meiotic recombination. *Nature*. 1997:386(6623):414–417. https://doi.org/10.1038/386414a0.

Bolívar P, Mugal CF, Nater A, Ellegren H. Recombination rate variation modulates gene sequence evolution mainly via GC-biased gene conversion, not Hill–Robertson interference, in an avian system. *Mol Biol Evol*. 2016:33(1):216–227. https://doi.org/10.1093/molbev/msv214.

Bomblies K, Jones G, Franklin C, Zickler D, Kleckner N. The challenge of evolving stable polyploidy: could an increase in "crossover interference distance" play a central role? *Chromosoma*. 2016:125(2):287–300. https://doi.org/10.1007/s00412-015-0571-4.

Botero-Castro F, Figuet E, Tilak M-K, Nabholz B, Galtier N. Avian genomes revisited: hidden genes uncovered and the rates versus traits paradox in birds. *Mol Biol Evol*. 2017:34(12):3123–3131. https://doi.org/10.1093/molbev/msx236.

Brand CL, Cattani MV, Kingan SB, Landeen EL, Presgraves DC. Molecular evolution at a meiosis gene mediates species differences in the rate and patterning of recombination. *Curr Biol*. 2018:28(8):1289–1295.e4. https://doi.org/10.1016/j.cub.2018.02.056.

Brandvain Y, Coop G. Scrambling eggs: meiotic drive and the evolution of female recombination rates. *Genetics*. 2012:190(2):709–723. https://doi.org/10.1534/genetics.111.136721.

Brekke C, Berg P, Gjuvsland AB, Johnston SE. Recombination rates in pigs differ between breeds, sexes and individuals, and are associated with the RNF212, SYCP2, PRDM7, MEI1 and MSH4 loci. *Genet Sel Evol*. 2022:54(1):33. https://doi.org/10.1186/s12711-022-00723-9.

Brooks LD, Marks RW. The organization of genetic variation for recombination in *Drosophila melanogaster*. *Genetics*. 1986:114(2):525–547. https://doi.org/10.1093/genetics/114.2.525.

Burt A, Bell G. Mammalian chiasma frequencies as a test of two theories of recombination. *Nature*. 1987:326(6115):803–805. https://doi.org/10.1038/326803a0.

Cannavo E, Sanchez A, Anand R, Ranjha L, Hugener J, Adam C, Acharya A, Weyland N, Aran-Guiu X, Charbonnier J-B, *et al*. Regulation of the MLH1–MLH3 endonuclease in meiosis. *Nature*. 2020:586(7830):618–622. https://doi.org/10.1038/s41586-020-2592-2.

Carballo GB, Honorato JR, de Lopes GPF, Spohr TCLS. A highlight on sonic hedgehog pathway. *Cell Commun Signal*. 2018:16(1):11. https://doi.org/10.1186/s12964-018-0220-7.

Carlisle E, Janis CM, Pisani D, Donoghue PCJ, Silvestro D. A timescale for placental mammal diversification based on Bayesian modeling of the fossil record. *Curr Biol*. 2023:33(15):3073–3082.e3. https://doi.org/10.1016/j.cub.2023.06.016.

Castresana J. Selection of conserved blocks from multiple alignments for their use in phylogenetic analysis. *Mol Biol Evol*. 2000:17(4):540–552. https://doi.org/10.1093/oxfordjournals.molbev.a026334.

Cavassim MIA, Baker Z, Hoge C, Schierup MH, Schumer M, Przeworski M. PRDM9 losses in vertebrates are coupled to those of paralogs ZCWPW1 and ZCWPW2. *Proc Natl Acad Sci U S A*. 2022:119(9):e2114401119. https://doi.org/10.1073/pnas.2114401119.

Charlesworth B, Morgan MT, Charlesworth D. The effect of deleterious mutations on neutral molecular variation. *Genetics*. 1993:134(4):1289–1303. https://doi.org/10.1093/genetics/134.4.1289.

Charlesworth J, Eyre-Walker A. The McDonald–Kreitman test and slightly deleterious mutations. *Mol Biol Evol*. 2008:25(6):1007–1015. https://doi.org/10.1093/molbev/msn005.

Chowdhury R, Bois PRJ, Feingold E, Sherman SL, Cheung VG. Genetic analysis of variation in human meiotic recombination. *PLoS Genet*. 2009:5(9):e1000648. https://doi.org/10.1371/journal.pgen.1000648.

Chuang Y-C, Smith GR. Meiotic crossover interference: methods of analysis and mechanisms of action. *Curr Top Dev Biol*. 2023:151:217–244. https://doi.org/10.1016/bs.ctdb.2022.04.006.

Civetta A, Singh RS. Broad-sense sexual selection, sex gene pool evolution, and speciation. *Genome*. 1999:42(6):1033–1041. https://doi.org/10.1139/g99-086.

Claramunt S, Cracraft J. A new time tree reveals Earth history's imprint on the evolution of modern birds. *Sci Adv*. 2015:1(11):e1501005. https://doi.org/10.1126/sciadv.1501005.

Cole F, Kauppi L, Lange J, Roig I, Wang R, Keeney S, Jasin M. Homeostatic control of recombination is implemented progressively in mouse meiosis. *Nat Cell Biol*. 2012:14(4):424–430. https://doi.org/10.1038/ncb2451.

Cole F, Keeney S, Jasin M. Evolutionary conservation of meiotic DSB proteins: more than just Spo11. *Genes Dev*. 2010:24(12):1201–1207. https://doi.org/10.1101/gad.1944710.

Comai L. The advantages and disadvantages of being polyploid. *Nat Rev Genet*. 2005:6(11):836–846. https://doi.org/10.1038/nrg1711.

Cook RD. Detection of influential observation in linear regression. *Technometrics*. 1977:19(1):15–18. https://doi.org/10.2307/1268249.

Cooney CR, Mank JE, Wright AE. Constraint and divergence in the evolution of male and female recombination rates in fishes. *Evolution*. 2021:75(11):2857–2866. https://doi.org/10.1111/evo.14357.

Damas J, Corbo M, Kim J, Turner-Maier J, Farré M, Larkin DM, Ryder OA, Steiner C, Houck ML, Hall S, *et al*. Evolution of the ancestral mammalian karyotype and syntenic regions. *Proc Natl Acad Sci U S A*. 2022:119(40):e2209139119. https://doi.org/10.1073/pnas.2209139119.

Dapper AL, Lively CM. Interlocus sexually antagonistic coevolution can create indirect selection for increased recombination. *Evolution*. 2014:68(4):1216–1224. https://doi.org/10.1111/evo.12338.

Dapper AL, Payseur BA. Connecting theory and data to understand recombination rate evolution. *Philos Trans R Soc Lond B Biol Sci*. 2017:372(1736):20160469. https://doi.org/10.1098/rstb.2016.0469.

Dapper AL, Payseur BA. Molecular evolution of the meiotic recombination pathway in mammals. *Evolution*. 2019:73(12):2368–2389. https://doi.org/10.1111/evo.13850.

Dapper AL, Wade MJ. The evolution of sperm competition genes: the effect of mating system on levels of genetic variation within and between species. *Evolution*. 2016:70(2):502–511. https://doi.org/10.1111/evo.12848.

Dapper AL, Wade MJ. Relaxed selection and the rapid evolution of reproductive genes. *Trends Genet*. 2020:36(9):640–649. https://doi.org/10.1016/j.tig.2020.06.014.

Degrandi TM, Barcellos SA, Costa AL, Garnero AD, Hass I, Gunski RJ. Introducing the bird chromosome database: an overview of cytogenetic studies in birds. *Cytogenet Genome Res*. 2020:160(4):199–205. https://doi.org/10.1159/000507768.

de Massy B. Initiation of meiotic recombination: how and where? Conservation and specificities among eukaryotes. *Annu Rev Genet*. 2013:47(1):563–599. https://doi.org/10.1146/annurev-genet-110711-155423.

de Vries SS, Baart EB, Dekker M, Siezen A, de Rooij DG, de Boer P, te Riele H. Mouse MutS-like protein Msh5 is required for proper chromosome synapsis in male and female meiosis. *Genes Dev*. 1999:13(5):523–531. https://doi.org/10.1101/gad.13.5.523.

Dumont BL, Broman KW, Payseur BA. Variation in genomic recombination rates among heterogeneous stock mice. *Genetics*. 2009:182(4):1345–1349. https://doi.org/10.1534/genetics.109.105114.

Dunwell TL, Paps J, Holland PWH. Novel and divergent genes in the evolution of placental mammals. *Proc Biol Sci*. 2017:284(1864):20171357. https://doi.org/10.1098/rspb.2017.1357.

Edgar RC. MUSCLE: multiple sequence alignment with high accuracy and high throughput. *Nucleic Acids Res*. 2004:32(5):1792–1797. https://doi.org/10.1093/nar/gkh340.

Ellegren H. Evolutionary stasis: the stable chromosomes of birds. *Trends Ecol Evol*. 2010:25(5):283–291. https://doi.org/10.1016/j.tree.2009.12.004.

Eyre-Walker A, Keightley PD. Estimating the rate of adaptive molecular evolution in the presence of slightly deleterious mutations and population size change. *Mol Biol Evol*. 2009:26(9):2097–2108. https://doi.org/10.1093/molbev/msp119.

Fay JC, Wyckoff GJ, Wu C-I. Positive and negative selection on the human genome. *Genetics*. 2001:158(3):1227–1234. https://doi.org/10.1093/genetics/158.3.1227.

Felsenstein J. *PHYLIP (Phylogeny Inference Package)*. Seattle: Distributed by the author, Department of Genome Sciences, University of Washington; 2005.

Ferguson-Smith MA, Trifonov V. Mammalian karyotype evolution. *Nat Rev Genet*. 2007:8(12):950–962. https://doi.org/10.1038/nrg2199.

Flexon PB, Rodell CF. Genetic recombination and directional selection for DDT resistance in *Drosophila melanogaster*. *Nature*. 1982:298(5875):672–674. https://doi.org/10.1038/298672a0.

Galtier N, Duret L. Adaptation or biased gene conversion? Extending the null hypothesis of molecular evolution. *Trends Genet*. 2007:23(6):273–277. https://doi.org/10.1016/j.tig.2007.03.011.

Gorlov I, Schuler L, Bunger L, Borodin P. Chiasma frequency in strains of mice selected for litter size and for high body weight. *Theor Appl Genet*. 1992:84(5-6):640–642. https://doi.org/10.1007/BF00224163.

Graphodatsky AS, Trifonov VA, Stanyon R. The genome diversity and karyotype evolution of mammals. *Mol Cytogenet*. 2011:4(1):22. https://doi.org/10.1186/1755-8166-4-22.

Gregory TR. Animal Genome Size Database: Home; 2024. [accessed 2024 Dec 12]. https://www.genomesize.com/.

Guiraldelli MF, Felberg A, Almeida LP, Parikh A, de Castro RO, Pezza RJ. SHOC1 is a ERCC4-(HhH)2-like protein, integral to the formation of crossover recombination intermediates during mammalian meiosis. *PLoS Genet*. 2018:14(5):e1007381. https://doi.org/10.1371/journal.pgen.1007381.

Halldorsson BV, Palsson G, Stefansson OA, Jonsson H, Hardarson MT, Eggertsson HP, Gunnarsson B, Oddsson A, Halldorsson GH, Zink F, *et al*. Characterizing mutagenic effects of recombination through a sequence-level genetic map. *Science*. 2019:363(6425):eaau1043. https://doi.org/10.1126/science.aau1043.

Haller BC, Messer PW. asymptoticMK: a web-based tool for the asymptotic McDonald–Kreitman test. *G3 (Bethesda)*. 2017:7(5):1569–1575. https://doi.org/10.1534/g3.117.039693.

Hassold T, Hunt P. To err (meiotically) is human: the genesis of human aneuploidy. *Nat Rev Genet*. 2001:2(4):280–291. https://doi.org/10.1038/35066065.

Hill WG, Robertson A. The effect of linkage on limits to artificial selection. *Genet Res (Camb)*. 1966:8(3):269–294. https://doi.org/10.1017/S0016672300010156.

Hinman AW, Yeh H-Y, Roelens B, Yamaya K, Woglar A, Bourbon H-MG, Chi P, Villeneuve AM. *Caenorhabditis elegans* DSB-3 reveals conservation and divergence among protein complexes promoting meiotic double-strand breaks. *Proc Natl Acad Sci U S A*. 2021:118(33):e2109306118. https://doi.org/10.1073/pnas.2109306118.

Huang Z, Furo IDO, Liu J, Peona V, Gomes AJB, Cen W, Huang H, Zhang Y, Chen D, Xue T, *et al*. Recurrent chromosome reshuffling and the evolution of neo-sex chromosomes in parrots. *Nat Commun*. 2022:13(1):944. https://doi.org/10.1038/s41467-022-28585-1.

Jaillon O, Aury J-M, Brunet F, Petit J-L, Stange-Thomann N, Mauceli E, Bouneau L, Fischer C, Ozouf-Costaz C, Bernot A, *et al*. Genome duplication in the teleost fish *Tetraodon nigroviridis* reveals the early

vertebrate proto-karyotype. *Nature*. 2004:431(7011):946–957. https://doi.org/10.1038/nature03025.
Jarvis ED, Mirarab S, Aberer AJ, Li B, Houde P, Li C, Ho SYW, Faircloth BC, Nabholz B, Howard JT, *et al.* Whole-genome analyses resolve early branches in the tree of life of modern birds. *Science*. 2014:346(6215):1320–1331. https://doi.org/10.1126/science.1253451.
Ji Z, Yao C, Yang C, Huang C, Zhao L, Han X, Zhu Z, Zhi E, Liu N, Zhou Z, *et al.* Novel hemizygous mutations of TEX11 cause meiotic arrest and non-obstructive azoospermia in Chinese Han population. *Front Genet*. 2021:12:741355. https://doi.org/10.3389/fgene.2021.741355.
Johnston SE, Bérénos C, Slate J, Pemberton JM. Conserved genetic architecture underlying individual recombination rate variation in a wild population of soay sheep (*Ovis aries*). *Genetics*. 2016:203(1):583–598. https://doi.org/10.1534/genetics.115.185553.
Johnston SE, Huisman J, Pemberton JM. A genomic region containing REC8 and RNF212B is associated with individual recombination rate variation in a wild population of red deer (*Cervus elaphus*). *G3 (Bethesda)*. 2018:8(7):2265–2276. https://doi.org/10.1534/g3.118.200063.
Jukes TH, Cantor CR. Evolution of protein molecules. In: *Mammalian protein metabolism*. Vol. 3. Cambridge, MA: Academic Press; 1969. p. 21–132.
Kadri NK, Harland C, Faux P, Cambisano N, Karim L, Coppieters W, Fritz S, Mullaart E, Baurain D, Boichard D, *et al.* Coding and non-coding variants in HFM1, MLH3, MSH4, MSH5, RNF212, and RNF212B affect recombination rate in cattle. *Genome Res*. 2016:26(10):1323–1332. https://doi.org/10.1101/gr.204214.116.
Kan F, Davidson MK, Wahls WP. Meiotic recombination protein Rec12: functional conservation, crossover homeostasis and early crossover/non-crossover decision. *Nucleic Acids Res*. 2011:39(4):1460–1472. https://doi.org/10.1093/nar/gkq993.
Kanaar R, Troelstra C, Swagemakers SMA, Essers J, Smit B, Franssen J-H, Pastink A, Bezzubova OY, Buerstedde J-M, Clever B, *et al.* Human and mouse homologs of the Saccharomyces cerevisiaeRAD54 DNA repair gene: evidence for functional conservation. *Curr Biol*. 1996:6(7):828–838. https://doi.org/10.1016/S0960-9822(02)00606-1.
Kapusta A, Suh A, Feschotte C. Dynamics of genome size evolution in birds and mammals. *Proc Natl Acad Sci U S A*. 2017:114(8):E1460–E1469. https://doi.org/10.1073/pnas.1616702114.
Keeney S. Mechanism and control of meiotic recombination initiation. *Curr Top Dev Biol*. 2001:52:1–53. https://doi.org/10.1016/S0070-2153(01)52008-6.
Keeney S. Spo11 and the formation of DNA double-strand breaks in meiosis. *Genome Dyn Stab*. 2008:2:81–123. https://doi.org/10.1007/7050_2007_026.
Keeney S, Giroux CN, Kleckner N. Meiosis-specific DNA double-strand breaks are catalyzed by Spo11, a member of a widely conserved protein family. *Cell*. 1997:88(3):375–384. https://doi.org/10.1016/s0092-8674(00)81876-0.
Kitayama S, Ikeda K, Sato W, Takeshita H, Kawakami S, Inoue S, Horie K. Testis-expressed gene 11 inhibits cisplatin-induced DNA damage and contributes to chemoresistance in testicular germ cell tumor. *Sci Rep*. 2022:12(1):18423. https://doi.org/10.1038/s41598-022-21856-3.
Kivikoski M, Rastas P, Löytynoja A, Merilä J. Predicting recombination frequency from map distance. *Heredity (Edinb)*. 2023:130(3):114–121. https://doi.org/10.1038/s41437-022-00585-3.
Kong A, Barnard J, Gudbjartsson DF, Thorleifsson G, Jonsdottir G, Sigurdardottir S, Richardsson B, Jonsdottir J, Thorgeirsson T, Frigge ML, *et al.* Recombination rate and reproductive success in humans. *Nat Genet*. 2004:36(11):1203–1206. https://doi.org/10.1038/ng1445.
Kong A, Thorleifsson G, Stefansson H, Masson G, Helgason A, Gudbjartsson DF, Jonsdottir GM, Gudjonsson SA, Sverrisson S, Thorlacius T, *et al.* Sequence variants in the RNF212 gene associate with genome-wide recombination rate. *Science*. 2008:319(5868):1398–1401. https://doi.org/10.1126/science.1152422.
Kuhl H, Frankl-Vilches C, Bakker A, Mayr G, Nikolaus G, Boerno ST, Klages S, Timmermann B, Gahr M. An unbiased molecular approach using 3′-UTRs resolves the avian family-level tree of life. *Mol Biol Evol*. 2021:38(1):108–127. https://doi.org/10.1093/molbev/msaa191.
Kulathinal RJ, Bennett SM, Fitzpatrick CL, Noor MAF. Fine-scale mapping of recombination rate in *Drosophila* refines its correlation to diversity and divergence. *Proc Natl Acad Sci U S A*. 2008:105(29):10051–10056. https://doi.org/10.1073/pnas.0801848105.
Kumar R, Bourbon H-M, de Massy B. Functional conservation of Mei4 for meiotic DNA double-strand break formation from yeasts to mice. *Genes Dev*. 2010:24(12):1266–1280. https://doi.org/10.1101/gad.571710.
Kumar S, Suleski M, Craig JM, Kasprowicz AE, Sanderford M, Li M, Stecher G, Hedges SB. TimeTree 5: an expanded resource for species divergence times. *Mol Biol Evol*. 2022:39(8):msac174. https://doi.org/10.1093/molbev/msac174.
Lamarche BJ, Orazio NI, Weitzman MD. The MRN complex in double-strand break repair and telomere maintenance. *FEBS Lett*. 2010:584(17):3682–3695. https://doi.org/10.1016/j.febslet.2010.07.029.
Larsson A. AliView: a fast and lightweight alignment viewer and editor for large datasets. *Bioinformatics*. 2014:30(22):3276–3278. https://doi.org/10.1093/bioinformatics/btu531.
Lartillot N, Poujol R. A phylogenetic model for investigating correlated evolution of substitution rates and continuous phenotypic characters. *Mol Biol Evol*. 2010:28(1):729–744. https://doi.org/10.1093/molbev/msq244. Coevol. [accessed 2024 Jun 13]. https://github.com/bayesiancook/coevol.
Lercher MJ, Hurst LD. Human SNP variability and mutation rate are higher in regions of high recombination. *Trends Genet*. 2002:18(7):337–340. https://doi.org/10.1016/S0168-9525(02)02669-0.
Letunic I, Bork P. Interactive Tree Of Life (iTOL) v5: an online tool for phylogenetic tree display and annotation. *Nucleic Acids Res*. 2021:49(W1):W293–W296. https://doi.org/10.1093/nar/gkab301.
Liu J, Wang X, Li J, Wang H, Wei G, Yan J. Reconstruction of the gene regulatory network involved in the sonic hedgehog pathway with a potential role in early development of the mouse brain. *PLoS Comput Biol*. 2014:10(10):e1003884. https://doi.org/10.1371/journal.pcbi.1003884.
Liu L, Zhang J, Rheindt FE, Lei F, Qu Y, Wang Y, Zhang Y, Sullivan C, Nie W, Wang J, *et al.* Genomic evidence reveals a radiation of placental mammals uninterrupted by the KPg boundary. *Proc Natl Acad Sci U S A*. 2017:114(35):E7282–E7290. https://doi.org/10.1073/pnas.1616744114.
Loidl J. Conservation and variability of meiosis across the eukaryotes. *Annu Rev Genet*. 2016:50:293–316. https://doi.org/10.1146/annurev-genet-120215-035100.
Lucaci AG, Wisotsky SR, Shank SD, Weaver S, Pond SLK. Extra base hits: widespread empirical support for instantaneous multiple-nucleotide changes. *PLoS One*. 2021:16(3):e0248337. https://doi.org/10.1371/journal.pone.0248337.
Ma L, O'Connell JR, VanRaden PM, Shen B, Padhi A, Sun C, Bickhart DM, Cole JB, Null DJ, Liu GE, *et al.* Cattle sex-specific recombination and genetic control from a large pedigree analysis. *PLoS Genet*. 2015:11(11):e1005387. https://doi.org/10.1371/journal.pgen.1005387.
Martin G, Otto S, Lenormand T. Selection for recombination in structured populations. *Genetics*. 2006:172(1):593–609. https://doi.org/10.1534/genetics.104.039982.
Martini E, Diaz RL, Hunter N, Keeney S. Crossover homeostasis in yeast meiosis. *Cell*. 2006:126(2):285–295. https://doi.org/10.1016/j.cell.2006.05.044.
McDonald JH, Kreitman M. Neutral mutation hypothesis test. *Nature*. 1991:354(6349):116. https://doi.org/10.1038/354116a0.
Meuwissen R, Offenberg H, Dietrich A, Riesewijk A, van Iersel M, Heyting C. A coiled-coil related protein specific for synapsed regions

of meiotic prophase chromosomes. *EMBO J.* 1992:11(13):5091–5100. https://doi.org/10.1002/j.1460-2075.1992.tb05616.x.

Miyata T, Yasunaga T. Molecular evolution of mRNA: a method for estimating evolutionary rates of synonymous and amino acid substitutions from homologous nucleotide sequences and its application. *J Mol Evol.* 1980:16(1):23–36. https://doi.org/10.1007/BF01732067.

Muñoz-Fuentes V, Marcet-Ortega M, Alkorta-Aranburu G, Linde Forsberg C, Morrell JM, Manzano-Piedras E, Söderberg A, Daniel K, Villalba A, Toth A, *et al.* Strong artificial selection in domestic mammals did not result in an increased recombination rate. *Mol Biol Evol.* 2015:32(2):510–523. https://doi.org/10.1093/molbev/msu322.

Myers S, Bowden R, Tumian A, Bontrop RE, Freeman C, MacFie TS, McVean G, Donnelly P. Drive against hotspot motifs in primates implicates the PRDM9 gene in meiotic recombination. *Science.* 2010:327(5967):876–879. https://doi.org/10.1126/science.1182363.

Nachman MW, Payseur BA. Recombination rate variation and speciation: theoretical predictions and empirical results from rabbits and mice. *Philos Trans R Soc Lond B Biol Sci.* 2012:367(1587):409–421. https://doi.org/10.1098/rstb.2011.0249.

Nam K, Mugal C, Nabholz B, Schielzeth H, Wolf JB, Backström N, Künstner A, Balakrishnan CN, Heger A, Ponting CP, *et al.* Molecular evolution of genes in avian genomes. *Genome Biol.* 2010:11(6):R68. https://doi.org/10.1186/gb-2010-11-6-r68.

Near TJ, Eytan RI, Dornburg A, Kuhn KL, Moore JA, Davis MP, Wainwright PC, Friedman M, Smith WL. Resolution of ray-finned fish phylogeny and timing of diversification. *Proc Natl Acad Sci U S A.* 2012:109(34):13698–13703. https://doi.org/10.1073/pnas.1206625109.

Oliver PL, Goodstadt L, Bayes JJ, Birtle Z, Roach KC, Phadnis N, Beatson SA, Lunter G, Malik HS, Ponting CP. Accelerated evolution of the Prdm9 speciation gene across diverse metazoan taxa. *PLoS Genet.* 2009:5(12):e1000753. https://doi.org/10.1371/journal.pgen.1000753.

Oliver TG, Grasfeder LL, Carroll AL, Kaiser C, Gillingham CL, Lin SM, Wickramasinghe R, Scott MP, Wechsler-Reya RJ. Transcriptional profiling of the Sonic hedgehog response: a critical role for N-myc in proliferation of neuronal precursors. *Proc Natl Acad Sci U S A.* 2003:100(12):7331–7336. https://doi.org/10.1073/pnas.0832317100.

Ortiz-Barrientos D, Engelstädter J, Rieseberg LH. Recombination rate evolution and the origin of species. *Trends Ecol Evol.* 2016:31(3):226–236. https://doi.org/10.1016/j.tree.2015.12.016.

Otto SP, Barton NH. Selection for recombination in small populations. *Evolution.* 2001:55(10):1921–1931. https://doi.org/10.1111/j.0014-3820.2001.tb01310.x.

Page SL, Hawley RS. The genetics and molecular biology of the synaptonemal complex. *Annu Rev Cell Dev Biol.* 2004:20:525–558. https://doi.org/10.1146/annurev.cellbio.19.111301.155141.

Paim LMG, FitzHarris G. Tetraploidy causes chromosomal instability in acentriolar mouse embryos. *Nat Commun.* 2019:10(1):4834. https://doi.org/10.1038/s41467-019-12772-8.

Parey E, Louis A, Montfort J, Guiguen Y, Crollius HR, Berthelot C. An atlas of fish genome evolution reveals delayed rediploidization following the teleost whole-genome duplication. *Genome Res.* 2022:32(9):1685–1697. https://doi.org/10.1101/gr.276953.122.

Parvanov ED, Petkov PM, Paigen K. Prdm9 controls activation of mammalian recombination hotspots. *Science.* 2010:327(5967):835. https://doi.org/10.1126/science.1181495.

Pavlova A, Gan HM, Lee YP, Austin CM, Gilligan DM, Lintermans M, Sunnucks P. Purifying selection and genetic drift shaped Pleistocene evolution of the mitochondrial genome in an endangered Australian freshwater fish. *Heredity (Edinb).* 2017:118(5):466–476. https://doi.org/10.1038/hdy.2016.120.

Petit M, Astruc J-M, Sarry J, Drouilhet L, Fabre S, Moreno CR, Servin B. Variation in recombination rate and its genetic determinism in sheep populations. *Genetics.* 2017:207(2):767–784. https://doi.org/10.1534/genetics.117.300123.

Pigozzi MI. Distribution of MLH1 foci on the synaptonemal complexes of chicken oocytes. *Cytogenet Cell Genet.* 2001:95(3-4):129–133. https://doi.org/10.1159/000059334.

Price MN, Dehal PS, Arkin AP. FastTree 2—approximately maximum-likelihood trees for large alignments. *PLoS One.* 2010:5(3):e9490. https://doi.org/10.1371/journal.pone.0009490.

Prum RO, Berv JS, Dornburg A, Field DJ, Townsend JP, Lemmon EM, Lemmon AR. A comprehensive phylogeny of birds (Aves) using targeted next-generation DNA sequencing. *Nature.* 2015:526(7574):569–573. https://doi.org/10.1038/nature15697.

Ptak SE, Hinds DA, Koehler K, Nickel B, Patil N, Ballinger DG, Przeworski M, Frazer KA, Pääbo S. Fine-scale recombination patterns differ between chimpanzees and humans. *Nat Genet.* 2005:37(4):429–434. https://doi.org/10.1038/ng1529.

Ratnakumar A, Mousset S, Glémin S, Berglund J, Galtier N, Duret L, Webster MT. Detecting positive selection within genomes: the problem of biased gene conversion. *Philos Trans R Soc Lond B Biol Sci.* 2010:365(1552):2571–2580. https://doi.org/10.1098/rstb.2010.0007.

Raynaud M, Sanna P, Joseph J, Clément J, Imai Y, Lareyre J-J, Laurent A, Galtier N, Baudat F, Duret L, *et al.* PRDM9 drives the location and rapid evolution of recombination hotspots in salmonid fish. *PLoS Biol.* 2025:23(1):e3002950. https://doi.org/10.1371/journal.pbio.3002950.

R Core Team. *R: a language and environment for statistical computing*. Vienna, Austria: R Foundation for Statistical Computing; 2023.

Reynolds A, Qiao H, Yang Y, Chen JK, Jackson N, Biswas K, Holloway JK, Baudat F, de Massy B, Wang J, *et al.* RNF212 is a dosage-sensitive regulator of crossing-over during mammalian meiosis. *Nat Genet.* 2013:45(3):269–278. https://doi.org/10.1038/ng.2541.

Ritz KR, Noor MAF, Singh ND. Variation in recombination rate: adaptive or not? *Trends Genet.* 2017:33(5):364–374. https://doi.org/10.1016/j.tig.2017.03.003.

Romanienko PJ, Camerini-Otero RD. The mouse Spo11 gene is required for meiotic chromosome synapsis. *Mol Cell.* 2000:6(5):975–987. https://doi.org/10.1016/s1097-2765(00)00097-6.

Ross-Ibarra J. The evolution of recombination under domestication: a test of two hypotheses. *Am Nat.* 2004:163(1):105–112. https://doi.org/10.1086/380606.

Rousselle M, Laverré A, Figuet E, Nabholz B, Galtier N. Influence of recombination and GC-biased gene conversion on the adaptive and nonadaptive substitution rate in mammals versus birds. *Mol Biol Evol.* 2019:36(3):458–471. https://doi.org/10.1093/molbev/msy243.

Sandor C, Li W, Coppieters W, Druet T, Charlier C, Georges M. Genetic variants in REC8, RNF212, and PRDM9 influence male recombination in cattle. *PLoS Genet.* 2012:8(7):e1002854. https://doi.org/10.1371/journal.pgen.1002854.

Segura J, Ferretti L, Ramos-Onsins S, Capilla L, Farré M, Reis F, Oliver-Bonet M, Fernández-Bellón H, Garcia F, Garcia-Caldés M, *et al.* Evolution of recombination in eutherian mammals: insights into mechanisms that affect recombination rates and crossover interference. *Proc R Soc Lond B Biol Sci.* 2013:280(1771):20131945. https://doi.org/10.1098/rspb.2013.1945.

Shen B, Jiang J, Seroussi E, Liu GE, Ma L. Characterization of recombination features and the genetic basis in multiple cattle breeds. *BMC Genomics.* 2018:19(1):304. https://doi.org/10.1186/s12864-018-4705-y.

Singh RS, Kulathinal RJ. Sex gene pool evolution and speciation: a new paradigm. *Genes Genet Syst.* 2000:75(3):119–130. https://doi.org/10.1266/ggs.75.119.

Singhal S, Leffler EM, Sannareddy K, Turner I, Venn O, Hooper DM, Strand AI, Li Q, Raney B, Balakrishnan CN, *et al.* Stable recombination hotspots in birds. *Science.* 2015:350(6263):928–932. https://doi.org/10.1126/science.aad0843.

Snowden T, Acharya S, Butz C, Berardini M, Fishel R. hMSH4-hMSH5 recognizes holliday junctions and forms a meiosis-specific sliding clamp that embraces homologous chromosomes. *Mol Cell.* 2004:15(3):437–451. https://doi.org/10.1016/j.molcel.2004.06.040.

Solovei I, Gaginskaya ER, Macgregor HC. The arrangement and transcription of telomere DNA sequences at the ends of lampbrush chromosomes of birds. *Chromosome Res*. 1994:2(6):460–470. https://doi.org/10.1007/BF01552869.

Song J, Sha Y, Liu X, Zeng X, Zhao X. Novel mutations of TEX11 are associated with non-obstructive azoospermia. *Front Endocrinol (Lausanne)*. 2023:14:1159723. https://doi.org/10.3389/fendo.2023.1159723.

Stapley J, Feulner PGD, Johnston SE, Santure AW, Smadja CM. Variation in recombination frequency and distribution across eukaryotes: patterns and processes. *Philos Trans R Soc Lond B Biol Sci*. 2017:372(1736):20160455. https://doi.org/10.1098/rstb.2016.0455.

Stoletzki N, Eyre-Walker A. Estimation of the neutrality Index. *Mol Biol Evol*. 2011:28(1):63–70. https://doi.org/10.1093/molbev/msq249.

Swanson WJ, Vacquier VD. The rapid evolution of reproductive proteins. *Nat Rev Genet*. 2002:3(2):137–144. https://doi.org/10.1038/nrg733.

Takezaki N. Global rate variation in bony vertebrates. *Genome Biol Evol*. 2018:10(7):1803–1815. https://doi.org/10.1093/gbe/evy125.

Tang L, Zeng W, Clark RK, Dobrinski I. Characterization of the porcine testis-expressed gene 11 (Tex11). *Spermatogenesis*. 2011:1(2):147–151. https://doi.org/10.4161/spmg.1.2.16680.

Tarsounas M, Morita T, Pearlman RE, Moens PB. Rad51 and dmc1 form mixed complexes associated with mouse meiotic chromosome cores and synaptonemal complexes. *J Cell Biol*. 1999:147(2):207–220. https://doi.org/10.1083/jcb.147.2.207.

Taylor JS, Braasch I, Frickey T, Meyer A, Van de Peer Y. Genome duplication, a trait shared by 22,000 species of ray-finned fish. *Genome Res*. 2003:13(3):382–390. https://doi.org/10.1101/gr.640303.

Tigano A, Khan R, Omer AD, Weisz D, Dudchenko O, Multani AS, Pathak S, Behringer RR, Aiden EL, Fisher H, *et al*. Chromosome size affects sequence divergence between species through the interplay of recombination and selection. *Evolution*. 2022:76(4):782–798. https://doi.org/10.1111/evo.14467.

Vaillant C, Monard D. SHH pathway and cerebellar development. *The Cerebellum*. 2009:8(3):291–301. https://doi.org/10.1007/s12311-009-0094-8.

Venkat A, Hahn MW, Thornton JW. Multinucleotide mutations cause false inferences of lineage-specific positive selection. *Nat Ecol Evol*. 2018:2(8):1280–1288. https://doi.org/10.1038/s41559-018-0584-5.

Volff J-N. Genome evolution and biodiversity in teleost fish. *Heredity (Edinb)*. 2005:94(3):280–294. https://doi.org/10.1038/sj.hdy.6800635.

von Wettstein D, Rasmussen SW, Holm PB. The synaptonemal complex in genetic segregation. *Annu Rev Genet*. 1984:18:331–411. https://doi.org/10.1146/annurev.ge.18.120184.001555.

Wang Q, Pierce-Hoffman E, Cummings BB, Alföldi J, Francioli LC, Gauthier LD, Hill AJ, O'Donnell-Luria AH, Karczewski KJ, MacArthur DG. Landscape of multi-nucleotide variants in 125,748 human exomes and 15,708 genomes. *Nat Commun*. 2020:11(1):2539. https://doi.org/10.1038/s41467-019-12438-5.

Waters PD, Patel HR, Ruiz-Herrera A, Álvarez-González L, Lister NC, Simakov O, Ezaz T, Kaur P, Frere C, Grützner F, *et al*. Microchromosomes are building blocks of bird, reptile, and mammal chromosomes. *Proc Natl Acad Sci U S A*. 2021:118(45):e2112494118. https://doi.org/10.1073/pnas.2112494118.

Xu H, Beasley MD, Warren WD, van der Horst GTJ, McKay MJ. Absence of mouse REC8 cohesin promotes Synapsis of sister chromatids in meiosis. *Dev Cell*. 2005:8(6):949–961. https://doi.org/10.1016/j.devcel.2005.03.018.

Yang F, Gell K, Heijden G, van der Eckardt SW, Leu NA, Page DC, Benavente R, Her C, Höög C, McLaughlin KJ, *et al*. Meiotic failure in male mice lacking an X-linked factor. *Genes Dev*. 2008:22(5):682–691. https://doi.org/10.1101/gad.1613608.

Yang F, Silber S, Leu NA, Oates RD, Marszalek JD, Skaletsky H, Brown LG, Rozen S, Page DC, Wang PJ. TEX11 is mutated in infertile men with azoospermia and regulates genome-wide recombination rates in mouse. *EMBO Mol Med*. 2015:7(9):1198–1210. https://doi.org/10.15252/emmm.201404967.

Yang Z. PAML 4: phylogenetic analysis by maximum likelihood. *Mol Biol Evol*. 2007:24(8):1586–1591. https://doi.org/10.1093/molbev/msm088.

Yang Z, Zou L, Sun T, Xu W, Zeng L, Jia Y, Jiang J, Deng J, Yang X. Genome-wide association study using whole-genome sequencing identifies a genomic region on chromosome 6 associated with comb traits in Nandan-Yao chicken. *Front Genet*. 2021:12:682501. https://doi.org/10.3389/fgene.2021.682501.

Yatsenko AN, Georgiadis AP, Röpke A, Berman AJ, Jaffe T, Olszewska M, Westernströer B, Sanfilippo J, Kurpisz M, Rajkovic A, *et al*. 2015. X-linked TEX11 mutations, meiotic arrest, and azoospermia in infertile men. *N Engl J Med*. 372(22):2097–2107. https://doi.org/10.1056/NEJMoa1406192.

Youds JL, Boulton SJ. The choice in meiosis—defining the factors that influence crossover or non-crossover formation. *J Cell Sci*. 2011:124(4):501–513. https://doi.org/10.1242/jcs.074427.

Yu X-C, Li M-J, Cai F-F, Yang S-J, Liu H-B, Zhang H-B. A new TEX11 mutation causes azoospermia and testicular meiotic arrest. *Asian J Androl*. 2021:23(5):510–515. https://doi.org/10.4103/aja.aja_8_21.

Yu Y-H, Siao F-P, Hsu LC-L, Yen PH. TEX11 modulates germ cell proliferation by competing with estrogen receptor β for the binding to HPIP. *Mol Endocrinol*. 2012a:26(4):630–642. https://doi.org/10.1210/me.2011-1263.

Yu Z, Vogel G, Coulombe Y, Dubeau D, Spehalski E, Hébert J, Ferguson DO, Masson JY, Richard S. The MRE11 GAR motif regulates DNA double-strand break processing and ATR activation. *Cell Res*. 2012b:22(2):305–320. https://doi.org/10.1038/cr.2011.128.

Zelkowski M, Olson MA, Wang M, Pawlowski W. Diversity and determinants of meiotic recombination landscapes. *Trends Genet*. 2019:35(5):359–370. https://doi.org/10.1016/j.tig.2019.02.002.

Zhang G, Li C, Li Q, Li B, Larkin DM, Lee CH, Lee CG, Storz JF, Antunes A, Greenwold MJ, *et al*. Comparative genomics reveals insights into avian genome evolution and adaptation. *Science*. 2014:346(6215):1311–1320. https://doi.org/10.1126/science.1251385.

Zhang N, Jiang Y, Mao Q, Demeler B, Tao YJ, Pati D. Characterization of the interaction between the cohesin subunits Rad21 and SA1/2. *PLoS One*. 2013:8(7):e69458. https://doi.org/10.1371/journal.pone.0069458.

Zheng Z, Zheng L, Arter M, Liu K, Yamada S, Ontoso D, Kim S, Keeney S. Reconstitution of SPO11-dependent double-strand break formation. *Nature*. 2025:639:784–791. https://doi.org/10.1038/s41586-025-08601-2.

Zhou Y, Shen B, Jiang J, Padhi A, Park K-E, Oswalt A, Sattler CG, Telugu BP, Chen H, Cole JB, *et al*. Construction of PRDM9 allele-specific recombination maps in cattle using large-scale pedigree analysis and genome-wide single sperm genomics. *DNA Res*. 2018:25(2):183–194. https://doi.org/10.1093/dnares/dsx048.